Palaeogeography, Palaeoclimatology, Palaeoecology 677 (2025) 113173

Contents lists available at ScienceDirect

Palaeogeography, Palaeoclimatology, Palaeoecology

journal homepage: www.elsevier.com/locate/palaeo

Oregon Oligo-Miocene herbivore community structure: Insights from morphology and stable isotope analysis

Dana M. Reuter [a,b,c,d,*], Jensen M. Wainwright [e], Jonathan M. Hoffman [f], Mark T. Clementz [g], Scott A. Blumenthal [e,h], Samantha S.B. Hopkins [a,b]

[a] Department of Earth Sciences, University of Oregon, Eugene, OR 97403, USA
[b] Museum of Natural and Cultural History, University of Oregon, Eugene, OR 97403, USA
[c] Florida Museum of Natural History, University of Florida, Gainesville, FL 32611, USA
[d] Texas A&M University, Department of Ecology and Conservation Biology, College Station, TX 77843, USA
[e] Department of Anthropology, University of Oregon, Eugene, OR 97403, USA
[f] Santa Barbara Museum of Natural History, Santa Barbara, CA 93105, USA
[g] Department of Geology & Geophysics, University of Wyoming, Laramie, WY 82071, USA
[h] Department of Earth, Ocean and Atmospheric Sciences, University of British Columbia, Vancouver, BC V6T 1Z4, Canada

ARTICLE INFO

Keywords:
Paleoecology
Miocene
Diet
Ungulate
Community structure
Stable isotope analysis

ABSTRACT

Extant ungulates exhibit a wide range of niche-partitioning strategies to reduce competition. Niche partitioning is thought to facilitate species coexistence in highly diverse communities. However, how ungulates partitioned plant-food resources in the past and how those relationships changed over time in response to vegetation dynamics remains unclear. We present a synthesis of stable carbon and oxygen isotope compositions from newly analyzed ($n = 134$) and previously published ($n = 77$) fossil tooth enamel specimens from three Oregon Oligo-Miocene fossil assemblages (John Day, Mascall, and Rattlesnake Formations). We pair these data with body mass and tooth-crown height estimates to investigate ecological changes in Oregon's ungulate communities during the Oligo-Miocene (~32–5 Ma), a time when grassland expansion coincided with significant changes in North American ungulate diversity. We find isotopic evidence that ungulates partitioned food resources in C_3-dominated ecosystems, particularly before and during the Mid-Miocene Climatic Optimum (MMCO). In contrast, the post-MMCO Rattlesnake Formation ungulates consumed isotopically similar C_3 plants. Morphological evidence supports these shifts, with a transition from low-crowned to mesodont and hypsodont teeth and a decline in small-bodied taxa. This work underscores the value of integrating isotopic and morphological data to better understand the ecological evolution of extinct communities.

Editor: Howard Falcon-Lang

1. Introduction

Today, grass-dominated ecosystems cover a vast amount of the terrestrial realm. Much of their evolution and expansion occurred during the Oligo-Miocene (~30–5 Ma) (Strömberg, 2011). During this time, the global expansion of grass-dominated habitats coincided with dramatic changes in ungulate (hooved mammal) diversity and community compositions (Janis et al., 2000). Understanding the spatial and temporal differences of concurrent animal community evolution during this time period has led to a greater understanding of the development of today's ecosystems. Despite the clear global trend of increased grass prevalence through the Miocene, local records show that there was a significant amount of heterogeneity in the timing of these vegetation changes (Strömberg, 2011; Strömberg and Staver, 2022) with local environmental factors influencing habitat change (Chen et al., 2015). For instance, in North America, the influence of geological features on precipitation patterns likely played a large role in determining when and where grass-dominated habitats would develop. Stable oxygen isotope measurements from authigenic clays and soil carbonates suggest that winter precipitation likely had previously supported more forested floras in the Great Plains (Kukla et al., 2022). The percentage of grass phytoliths in the Great Plains sedimentary record dramatically increases between 26 and 15 Ma (Kukla et al., 2022) with phytolith composition indicating a mix of grassy and wooded patches in the middle Miocene

* Corresponding author at: Cascade Hall 100, 1272, University of Oregon, Eugene, OR 97403, USA.
E-mail address: dreuter@uoregon.edu (D.M. Reuter).

https://doi.org/10.1016/j.palaeo.2025.113173
Received 25 April 2025; Received in revised form 29 July 2025; Accepted 30 July 2025
Available online 5 August 2025

and greater dominance of grasses during the latest Miocene (Strömberg, 2011). In contrast with the Great Plains, the west coast even today boasts densely forested areas and saw less of a change in winter precipitation during the Miocene (Kukla et al., 2022).

The changing vegetation greatly influenced ungulate diversity during the Oligo-Miocene, with ungulate diversity being highest around the Mid-Miocene Climatic Optimum (MMCO, ~16 Ma) (Janis et al., 2000). After 16 Ma, global temperatures decreased, grasslands spread, and ungulate diversity fell and continued to decline as the Miocene progressed (Barry, 1995; Janis et al., 2000, 2002, 2004). Ungulates with low-crowned teeth, which have been shown to have narrower diets than ungulates with higher crowned teeth (Feranec, 2003; Feranec, 2007a, 2007b; Pardi and DeSantis, 2021), decreased in diversity the most (Janis et al., 2000). Many browsing taxa were lost completely, such as members of Merycoidodontoidea, a previously diverse clade endemic to North America (Janis et al., 1998). These changes ultimately contributed to the structure of modern ungulate communities, which are characterized by low diversity and low abundance in browsing taxa. Timing of these faunal adaptations to the changing environments, however, might also reflect the regional heterogeneity seen in the records of grassland expansion (Strömberg, 2011).

In extant species-rich herbivore communities, ungulates partition food resources, which potentially lowers interspecific competition and allows for higher diversity (Kartzinel et al., 2015; Pansu et al., 2022). The MMCO communities containing especially high species richness in browsing ungulates suggest a degree of resource partitioning that was different from today's depauperate ecosystems (Janis et al., 2000). Additionally, increased niche overlap estimates between extant grazing species indicate that resource partitioning differs between open grassy environments and densely wooded environments (Pansu et al., 2022). Given the heightened diversity of browsing organisms and subsequent decline during the Miocene, it is likely that ungulate niche partitioning shifted as vegetation and community composition changed. Understanding the potential diets and spatial use of extinct Miocene herbivores will help us understand: 1) if ungulate niche partitioning reflects modern patterns, and 2) how ungulate communities changed and evolved in response to the occurring climatic and vegetation change.

The extensive fossil record of Oregon is ideal for expanding our knowledge of Miocene changes in ungulate diversity and ecology. Previous work has suggested that Oregon follows many of the same environmental and vegetation trends seen elsewhere in North America, with species diversity decreasing after the MMCO (Kohn and Fremd, 2007). However, paleosol evidence suggests that during the MMCO Oregon received more rainfall than the Great Plains (Bestland et al., 2008). Additionally, unlike the Great Plains, Oregon has a long history of tectonic activity. During the Oligo-Miocene the Cascades were uplifted (Bershaw et al., 2019; Pesek et al., 2020), the large Columbia River flood basalts were deposited (Reidel et al., 2013; Cahoon et al., 2020), and Basin and Range extension propagated into the state (Dickinson, 2002). Work on modern mammals and fossil assemblages have shown that areas with complex topography have higher species richness because they provide a higher variety of habitats (Badgley et al., 2017; Badgley et al., 2017; Loughney et al., 2021; Smiley et al., 2024). It has been hypothesized that the combination of tectonic changes in topography and climate change during the MMCO increased habitat and species richness in Oregon (Kohn and Fremd, 2007). The long history of tectonic and volcanic events in Oregon makes it a key place for expanding our understanding of how ungulate diversity and community structure changed during the Oligo-Miocene. Ungulate diversity in Oregon could have changed differently than Great Plains communities given the additional forcings from topographic change, less extreme precipitation changes, and potentially more heterogeneous environments.

In this study we use stable carbon and oxygen isotope analyses of tooth enamel from three Oregon fossil assemblages, to reconstruct ungulate ecology, resource partitioning, and isotopic niche breadth. Stable isotope work can give a more detailed picture of ungulate diet than tooth morphology alone and can provide a picture of how niche partitioning changed as browser diversity fell. Additionally, morphology used in conjunction with fossil enamel stable isotope compositions has proven to be a useful method for identifying dietary-niche differences and partitioning in co-occurring extinct taxa, allowing for insights into the evolutionary changes that have led to our current herbivore community (Bibi, 2007; Pardi and DeSantis, 2021). This study expands on previous isotopic work on Oregon fossil mammals (Maguire, 2015; Drewicz and Kohn, 2018), which mostly focused on equids. Specifically, we are interested in answering the following questions: 1. Is there isotopic evidence that Oregon Oligo-Miocene ungulate species partitioned available plant-food resources in a purely C_3 environment? 2. Did dietary diversity and/or niche partitioning change through the Oligo-Miocene?

2. Materials and methods

2.1. Specimens

We present a compilation of new ($n = 134$) and previously published ($n = 77$) tooth enamel $\delta^{13}C$ (Maguire, 2015; Drewicz and Kohn, 2018) from fossil specimens representing 29 taxa from the John Day Formation Turtle Cove Member (~32–26 Ma; Fisher and Rensberger, 1972; Albright III et al., 2008; Mohr et al., 2025), the Mascall Formation (~16–13 Ma; Maguire et al., 2018), and the Rattlesnake Formation (~7.3–6.9 Ma; Streck and Grunder, 1995; Prothero et al., 2006). The geographical and temporal position of the formations included in this analysis are shown in Fig. 1. We present $\delta^{18}O$ values for the unpublished analyzed enamel samples (n = 134). We refrain from aggregating previously published $\delta^{18}O$ into our analyses as many of the previously published values were not corrected for the temperature-dependent isotopic fractionation between CO_2 and tooth enamel carbonate, which is known to affect comparability (Passey et al., 2007). Methodological and condition differences between labs have been shown to result in different $\delta^{18}O$ results and could lead to incorrect interpretations (Chesson et al., 2019; Pestle et al., 2014).

New measurements for this study were taken from fossil material housed in both the Museum of Natural and Cultural History (UOMNH) and the John Day Fossil Beds National Monument (JODA). In total, our analyses include previously published and new isotopic measurements from 211 specimens. Complete specimen details, isotopic values, and specimen publication details can be found in Supplemental material 1.

The stable isotope data reported in this study include teeth sampled by one of the authors (D.R.) and analyzed in the University of Oregon Stable Isotope Laboratory in 2021 as well as teeth sampled by one of us (J.H.) and analyzed in the University of Wyoming Stable Isotope Facility in 2010. Given that stable isotope analysis is destructive and some of the ungulates from these formations have thin enamel, all but one specimen included in the initial University of Wyoming study were not re-sampled.

2.2. Sampling, pretreatment, and isotope analysis

Enamel samples were collected from fossil teeth using a rotary hand drill with a diamond bit, removing ~3–4 mg of powdered enamel. We prioritized sampling from a previously damaged or non-diagnostic region of the tooth. Broken teeth, while sometimes being not as diagnostic for species identification, provide the added benefit of more easily distinguishing enamel from dentin, or matrix. This sampling approach also reduces impact on the fossil collections by sampling regions that can't be used for microwear or morphological analysis.

Tooth enamel samples ($n = 91$) analyzed at the University of Oregon Stable Isotope Laboratory were pretreated for 15 min. Using 0.1 M buffered acetic acid to remove any secondary carbonate, following methods outlined in Koch et al. (1997) and Pellegrini and Snoeck (2016). Following pretreatment, samples were rinsed to neutrality using Type 1 ultrapure water, dried overnight at 60 °C. Approximately 600 μg

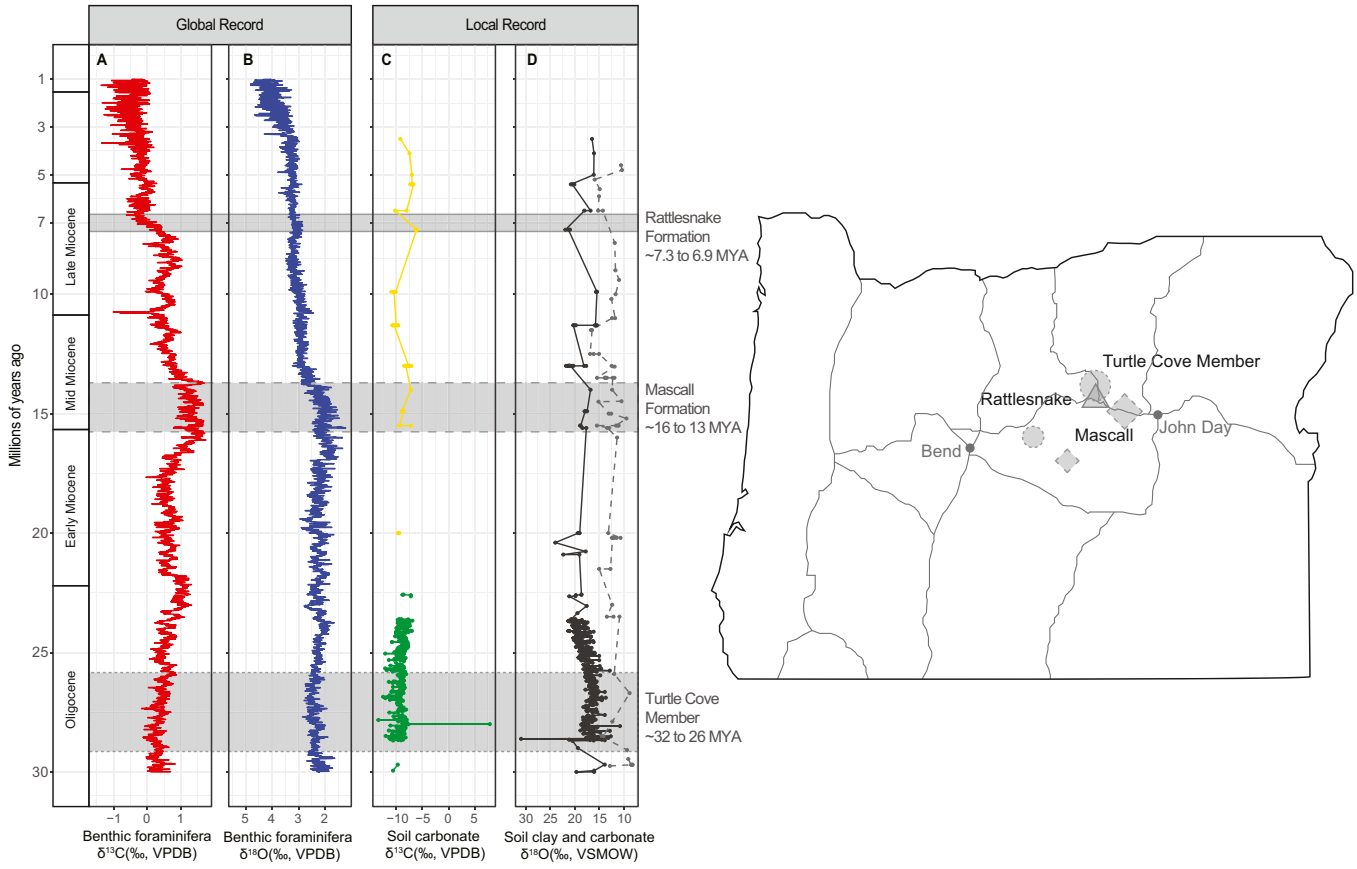

Fig. 1. Global trend and fossil localities

Global and local isotopic records for the last 30 million years. Gray boxes represent the geochronological sequence and geographic location of the formations included in this study. Map of Oregon shows the geographic location of the formations included in this study, with John Day Formation Turtle Cove Member localities represented by circles, Mascall Formation localities represented by diamonds, and the Rattlesnake locality represented by a triangle. (A) Benthic foraminifera stable carbon isotope dataset from Westerhold et al. 2020. (B) Benthic foraminifera stable oxygen dataset from Westerhold et al. 2020. (C) Compiled soil carbonate stable carbon isotope data. Yellow line represents data from Takeuchi et al., 2010 and green line represents data from Retallack et al. 2004. (D) Compiled stable oxygen dataset from Kukla et al., 2022. Solid line represents data from soil carbonate samples and the dashed line represents data from clay samples. (For interpretation of the references to colour in this figure legend, the reader is referred to the web version of this article.)

of enamel powder was added to 4.5 ml Exetainer vials, and CO_2 was liberated from pretreated tooth enamel via a 1-h phosphoric acid (H_3PO_4) digestion at 70 °C. Liberated CO_2 was analyzed using a Thermo Gas Bench II coupled with a Thermo MAT 253 isotope ratio mass spectrometer in the University of Oregon Stable Isotope Laboratory. Temperature dependence of oxygen isotopic acid fractionation was corrected for (Passey et al., 2007) using apparent fractionation factors (α*) reported in Kusaka and Nakano (2014). Stable isotope ratios were normalized to the Vienna Pee Dee Belemnite (VPDB) scale using internal calcite and tooth enamel reference materials that were analyzed alongside the samples for each run. Analytical reproducibility is indicated by the standard deviation of the standards (Carrara marble, USGS-44, IAEA-CO-8, FBS, MBS), which was 0.2 ‰ for both $\delta^{13}C$ and $\delta^{18}O$.

Tooth enamel samples (n = 43) analyzed at the University of Wyoming Stable Isotope Facility were pretreated with 30 % hydrogen peroxide to remove organics and 0.1 M buffered acetic acid to remove secondary carbonate, following the methods of Koch et al. (1997). Samples were rinsed with deionized water, freeze dried, and at least 700 μg to was placed into headspace vials that were subsequently flushed with helium. These specimens were allowed to react with phosphoric acid for 24 to 48 h at room temperature prior to the liberated CO_2 being analyzed using a Thermo Gas Bench II coupled with a Thermo Finnigan DeltaPlus XP Continuous Flow stable isotope ratio mass spectrometer. We assume that temperature dependent acid fractionation of tooth enamel is the same as the calcite standards for reactions at room temperature (i.e. temperatures near 25 °C) (Passey et al., 2007; Chesson et al., 2019). Carbon and oxygen isotope ratios were normalized to Vienna Pee Dee Belemnite (VPDB) using calcite lab standards (UWSIF 18 and UWSIF 06). Reproducibility is indicated by the standard deviation of standards (NBS-120C, UWSIF 17, UWSIF 18, UWSIF 06) analyzed alongside the fossil samples, which was 0.2 ‰ for both $\delta^{13}C$ and $\delta^{18}O$.

Isotopic data are reported in standard delta (‰) notation:

$$\delta^{13}C = \left[\left(R_{sample}/R_{standard}\right) - 1\right] \times 1000$$

Where R is the ratio of the abundance of the heavy and light isotopes.

2.3. Isotopic ecological interpretations

2.3.1. Predicting carbon isotope values for Oligo-Miocene mammals

The carbon isotope composition in plants depends on the photosynthetic pathway used by specific plant species. C_3 plants, which photosynthesize using the Calvin Cycle, have a mean $\delta^{13}C$ value of approximately −28.5 ‰ and include many trees, herbs, and cool-growing-season grasses (Ehleringer et al., 1991; Kohn, 2010). C_4 plants, which include warm-growing-season grasses and sedges, photosynthesize carbon using the Hatch-Slack cycle and have a mean $\delta^{13}C$ value of approximately −13 ‰ (Ehleringer et al., 1991; Cerling et al., 1997). Among C_3 plants, carbon isotope variation is influenced by differences in light intensity, temperature, canopy cover, and water stress, resulting in a wide range in carbon isotope values ($\delta^{13}C$) from −20 ‰ to

−37 ‰ in plant tissues (Farquhar et al., 1989; Kohn, 2010), with lower $\delta^{13}C$ in closed, humid habitats and higher $\delta^{13}C$ in more dry and open habitats (Farquhar et al., 1989; Kohn, 2010). The variation in $\delta^{13}C$ values of C_3 plants makes it possible to reconstruct aspects of the diets of organisms that fed on C_3 plants (Cerling et al., 1997; Feranec, 2007a, 2007b). Previous stable carbon isotope analyses of extant ungulate tooth enamel have successfully detected diet variations among species in purely C_3 systems (Feranec, 2007a, 2007b), which is promising because Oregon has long been in a climatic zone that favors C_3 plants over C_4 plants (Ehleringer and Cerling, 2002) and past studies show no evidence for C_4 plants at these fossil localities (Drewicz and Kohn, 2018; Maguire, 2015). Tooth enamel is preferred for paleontological studies because it is more resistant to isotopic alteration (Koch, 2007). The carbon isotope composition of mammalian tooth enamel reflects the carbon isotope composition of diet during the period of tooth formation, and among medium- to large-bodied mammalian herbivores the carbon isotope enrichment between enamel and diet is 14.1 ± 0.5 ‰ (Cerling and Harris, 1999).

In this study, we use the $\delta^{13}C$ of fossil tooth enamel to evaluate the reliance of extinct mammals on dietary resources from closed canopy forests to open water-stressed C_3 ecosystems. For each fossil assemblage, we estimate $\delta^{13}C$ ranges for closed canopy, non-closed canopy C_3, and water-stressed C_3 environments, as well as the maximum dietary value given a purely C_3 environment. These estimated ranges are based on $\delta^{13}C$ of modern C_3 flora (Kohn, 2010) adjusted for diet-enamel enrichment (Cerling and Harris, 1999) and change in $\delta^{13}C$ of atmospheric CO_2 through geologic time (Tipple et al., 2010) (see Supplemental material 2 for details and calculations).

The expected carbon isotope composition of open and closed C_3 biomass can also depend on other factors, such as plant parts (Metcalfe, 2021), and the light intensity, temperature, and water stress they experience (Farquhar et al., 1989; Kohn, 2010; Metcalfe, 2021). Seeds and flowers have been shown to have elevated $\delta^{13}C$ compared to leaves (Metcalfe, 2021) and new leaves have elevated $\delta^{13}C$ compared to mature leaves (Vogado et al., 2020). Therefore, we cannot say that some of the isotopic differences found in our study are solely because the ungulates were eating plants in different microhabitats. Consumption of different plant parts, or different plants across microhabitats, could potentially result in similar isotopic enamel records. Eating plants in different habitats, eating different plant parts, or eating plant material at different foraging heights, are common resource partitioning strategies for ungulates to reduce competition and are important aspects of ungulate communities with high species richness (Pansu et al., 2022; Potter et al., 2022). Therefore, isotopic niches that we estimate likely represent many foraging strategies.

2.3.2. Oxygen isotopes in mammalian tooth enamel

The oxygen stable isotope composition of mammalian tooth enamel is mostly determined by the ingested water isotopic composition and the physiology and hydration requirements of the taxa (Bryant and Froelich, 1995; Kohn, 1996). Ungulates ingest water from two sources: meteoric water, or water from consumed plants. The $\delta^{18}O$ of meteoric water is determined by climate influences such as temperature and can shift through geologic time as global temperature and precipitation sources change (Rozanski et al., 1992; Fricke and O'Neil, 1999).

Within ecological communities, relative $\delta^{18}O$ can indicate the drinking habits of taxa (Levin et al., 2006). Some ungulates are considered obligate drinkers (e.g., modern horses and rhinos), as they obtain most of their water from available bodies of water, which usually have undergone minimal evaporation (Kohn, 1996). Other ungulates are considered drought-resistant or drought-tolerant (e.g., modern goats and gazelles), and either have physiological adaptations allowing them to drink less water or they obtain most of their ingested water from the plant material they consume (Kohn, 1996; Levin et al., 2006). Within a community, the tooth enamel $\delta^{18}O$ values will largely reflect these water consumption differences, with obligate drinkers having lower $\delta^{18}O$ values than drought-resistant species (Blumenthal et al., 2017; Faith, 2018; Kohn, 1996; Levin et al., 2006). This pattern is largely because leaf water will have higher $\delta^{18}O$ values due to increased evaporation from the leaf when compared to the surrounding meteoric water (Levin et al., 2006; Yakir et al., 1990). The leaf $\delta^{18}O$ enrichment due to evaporation increases as aridity and solar radiation increases.

2.3.3. Hypsodonty and estimating body mass

Morphology and past studies of tooth wear and microwear can inform which dietary strategy is most likely for a given organism within a community. Craniodental morphology has been shown to correlate with diet in ungulates and has been very useful when paired with other diet proxies (Mihlbachler et al., 2011; Pardi and DeSantis, 2021). To complement the isotopic data and provide a multiproxy understanding of the ecology of these extinct ungulates, we collected data on both the body mass and tooth crown height for each taxon. We used published sources (Janis et al., 2004) and the NOW database (New and Old Worlds Database of fossil mammals) (The NOW Community, 2024) to classify taxa as having as brachydont, mesodont, or hypsodont teeth. The classifications in Janis et al., 2004 and the NOW database are based on a hypodonty index calculated from the ratio of the lower third molar (m3) crown height and tooth width at the occlusal surface. Taxa with m3s that have a hypsodonty index of $\leq$1.5 are considered brachydont, hypsodonty index of 1.5–3 are considered mesodont, and hypsodonty index >3 are considered hypsodont (Janis, 1988). The NOW database draws from available published information (e.g., Janis et al., 1998) and but also uses the upper second molar (M2) for scoring dental characteristics when it is appropriate (Žliobaitė et al., 2016). Taxa listed as submesodont (i.e., *Ticholeptus* and *Merychippus*) in Janis et al. (2004) were categorized as mesodont because they were listed as mesodont in the NOW database. Body masses were reconstructed using the lower first molar (m1) area and regressions from Legendre (1986). All body mass reconstructions, except those for members of Rhinocerotidae, were done using the all-mammal regression equation. The body masses for members of Rhinocerotidae were reconstructed using the large-mammal regression equation after it was observed that their body mass reconstructions using the all-mammal equation were larger than expected. Data for the m1 area were compiled from the Paleobiology Database with additional information from published descriptions (see Supplemental material 3 for all for measurements, calculations, and references). If a species m1 was not available, other members of the genus or a genus average were used (see Supplemental material 3 for details).

2.4. Data analysis

All statistical analyses and data visualizations were performed using the 'R' statistical software version 4.3.2 (R Core Team, 2023). Levene's test was used to test for differences in variance before selecting parametric or non-parametric methods for comparisons ('car' package; Fox and Weisberg, 2019). To compare formations to one another we performed one-factor analysis of variance (ANOVA) followed by a post hoc Tukey test which provided pairwise comparisons between the formations ('stats' package; R Core Team, 2023). To test for isotopic niche partitioning between taxa in a formation we used ANOVAs and post hoc Tukey tests to test for differences in mean $\delta^{13}C$. We used non-parametric Kruskal-Wallis rank sum test and a following Wilcoxon rank-sum test for communities whose taxa had significantly different variance ('stats' package; R Core Team, 2023).

3. Results

Summary statistics for individual taxa from the combined $\delta^{13}C$ data from this study, Maguire (2015), and Drewicz and Kohn (2018) can be found in Table 1. Fig. 2 shows all $\delta^{13}C$ measurements in relation to estimated diets in closed-canopy to water-stressed C_3 environments. Number of specimens sampled, median, mean and standard deviation of

Table 1
Mean $\delta^{13}C$ (‰), S.D. $\delta^{13}C$ (‰), and number of specimens measured for this study, Maguire, 2015, and Drewicz and Kohn, 2018.

Formation	Taxon	$\delta^{13}C$ (‰) n	Mean $\delta^{13}C$ (‰)	S.D. $\delta^{13}C$ (‰)	Max $\delta^{13}C$ (‰)	Min $\delta^{13}C$ (‰)
Rattlesnake	*Hipparion*	6	−10.53	0.68	−9.4	−11.5
Rattlesnake	*Pliohippus*	9	−10.52	0.63	−9.8	−11.6
Rattlesnake	Antilocapridae	13	−9.86	1.00	−8.5	−11.5
Rattlesnake	Camelidae	4	−11.10	0.80	−10.1	−11.8
Rattlesnake	Tayassuidae	7	−10.89	0.76	−9.5	−11.9
Rattlesnake	Rhinocerotidae	9	−10.56	0.89	−9.4	−12.2
Rattlesnake	*Neohipparion*	1	−9.90	NA	NA	NA
Mascall	Tayassuidae	1	−8.30	NA	NA	NA
Mascall	*Archaeohippus*	9	−8.87	0.77	−7.1	−9.9
Mascall	*Dromomeryx*	8	−10.26	1.06	−8.7	−11.9
Mascall	*Acritohippus*	6	−10.92	0.90	−9.9	−12.5
Mascall	*Ticholeptus*	9	−11.33	1.51	−9.3	−13.1
Mascall	Rhinocerotidae	6	−10.05	0.88	−9.4	−11.7
Mascall	*Merychippus*	51	−10.55	0.82	−8.82	−12.4
Mascall	*Parahippus*	7	−10.79	0.92	−9.29	−11.74
Mascall	*Desmatippus*	3	−10.32	0.29	−9.99	−10.56
Mascall	*Blastomeryx*	1	−9.50	NA	NA	NA
Turtle Cove	Tayassuidae	6	−9.65	1.06	−8.3	−11.2
Turtle Cove	*Miohippus*	9	−10.01	0.91	−8.7	−11.8
Turtle Cove	*Hypertragulus*	2	−10.70	0.71	−10.2	−11.2
Turtle Cove	*Eporeodon*	8	−12.30	0.86	−10.7	−13.4
Turtle Cove	*Archaeotherium*	8	−11.38	1.28	−9.3	−13
Turtle Cove	*Diceratherium*	12	−10.33	0.81	−9	−11.5
Turtle Cove	*Agriochoerus*	5	−10.68	0.59	−10.1	−11.6
Turtle Cove	*Mesohippus*	3	−10.83	0.61	−10.3	−11.5
Turtle Cove	*Nanotragulus*	3	−10.87	0.32	−10.5	−11.1
Turtle Cove	*Paroreodon*	2	−11.20	0.99	−10.5	−11.9
Turtle Cove	*Merycoidodont*	3	−13.20	1.35	−11.9	−14.6

the combined $\delta^{13}C$ and $\delta^{18}O$ separated by formation can be found in Table 2.

3.1. Family level summaries

3.1.1. Tayassuidae

In total, fourteen tayassuid teeth were sampled for this study, seven from the Rattlesnake Formation, six from the John Day Formation, and one from the Mascall Formation. $\delta^{13}C$ values range from −11.9 ‰ to −8.3 ‰. The highest $\delta^{13}C$ value was observed both in the John Day specimens (−8.3 ‰), and the single Mascall specimen (−8.3 ‰). $\delta^{18}O$ values range from −9.8 ‰ to −3.5 ‰.

3.1.2. Entelodontidae

Eight *Archaeotherium* specimens from the John Day Formation were sampled for this study. They show a wide range of $\delta^{13}C$ values, from −13.0 ‰ to −9.3 ‰ (mean = −11.4 ± 1.3 ‰), the widest $\delta^{13}C$ range recorded within a single taxon across all formations (3.7 ‰). $\delta^{18}O$ values range from −8.4 ‰ to −5.4 ‰.

3.1.3. Merycoidodontoidea

Nineteen specimens were sampled for this study resulting in a total of twenty-seven Merycoidodontoid specimens in the combined $\delta^{13}C$ dataset (Drewicz and Kohn, 2018). The $\delta^{13}C$ values for all Merycoidodontoid specimens range from −14.6 ‰ to −9.3 ‰. These include *Agriochoerus antiquus* (n = 5), *Eporeodon* (n = 8), *Paroreodon* (n = 2), unidentified merycoidodonts (n = 3) from the John Day Formation, and *Ticholeptus* (n = 9) from the Mascall Formation. $\delta^{18}O$ values range from −10.3 ‰ to −1 ‰.

3.1.4. Hypertragulidae

Five specimens were sampled for this study from the John Day Formation and yielded $\delta^{13}C$ values ranging from −11.2 ‰ to −10.2 ‰ and $\delta^{18}O$ values ranging from −6.2 ‰ to −3 ‰.

3.1.5. Dromomerycidae/Moschidae

Eight *Dromomeryx* specimens and one *Blastomeryx* specimen were sampled for this study from the Mascall Formation. In the combined dataset, $\delta^{13}C$ values for Dromomeryx range from −11.9 ‰ to −8.7 ‰ with a mean of −10.3 ± 1.1 ‰. The single *Blastomeryx* specimen recorded a $\delta^{13}C$ value of −9.5 ‰. $\delta^{18}O$ values range from −10 ‰ to −3.5 ‰ for *Dromomeryx* and the single *Blastomeryx* sample had a $\delta^{18}O$ value of −10 ‰.

3.1.6. Antilocapridae

Thirteen Antilocapridae teeth were sampled for this study, all from the Rattlesnake Formation. $\delta^{13}C$ values range from −11.5 ‰ to −8.5 ‰, with a mean of −9.9 ± 1.0 ‰. They also have the highest $\delta^{13}C$ values in the Rattlesnake assemblage. $\delta^{18}O$ values range from −11.1 ‰ to −2.1 ‰.

3.1.7. Camelidae

Four camelid specimens were sampled for this study, all from the Rattlesnake Formation. $\delta^{13}C$ values for Camelidae range from −11.8 ‰ to −10.1 ‰, with a mean of −11.1 ± 0.8 ‰. $\delta^{18}O$ values for these specimens range from −9.1 ‰ to −6.3 ‰.

3.1.8. Equidae

Thirty-nine equid specimens were sampled for this study, contributing to a total of one hundred and four equid specimens in the combined $\delta^{13}C$ dataset (includes data from Maguire, 2015 and Drewicz and Kohn, 2018). These specimens represent ten genera: *Mesohippus* (n = 3), *Miohippus* (n = 9) from the John Day Formation, *Acritohippus* (n = 6), *Archaeohippus* (n = 9), *Desmatippus* (n = 3), *Parahippus* (n = 7), and *Merychippus* (n = 51) from the Mascall Formation, and *Pliohippus* (n = 9), *Neohipparion* (n = 1), and *Hipparion* (n = 6) from the Rattlesnake Formation. In terms of $\delta^{13}C$, values range from −12.5 ‰ (*Acritohippus*) to −7.1 ‰ (*Archaeohippus*). The highest mean $\delta^{13}C$ value is observed in *Archaeohippus* (−8.9 ± 0.8 ‰, n = 9), while the lowest mean is in *Acritohippus* (−10.9 ± 0.9 ‰, n = 6). $\delta^{18}O$ values range from −12.3 ‰ (*Pliohippus*) to −2.6 ‰ (*Archaeohippus*).

3.1.9. Rhinocerotidae

Twenty-three specimens were sampled for this study, contributing to a total of twenty-seven rhinocerotid specimens in the combined dataset, encompassing individuals identified as either *Diceratherium* or more generally as Rhinocerotidae. These specimens are distributed across three formations: Turtle Cove (n = 12), Rattlesnake (n = 9), and Mascall (n = 6). $\delta^{13}C$ values range from −12.2 ‰ to −9.0 ‰. The lowest $\delta^{13}C$ value is from a Rattlesnake Formation specimen. $\delta^{18}O$ values range from −12.5 ‰ to −4.0 ‰.

3.2. Formation comparisons

Among all fossil mammals, $\delta^{13}C$ values show a range of −14.6 ‰ to −8.3 ‰ for the John Day Formation (n = 62, 11 taxa), −13.1 ‰ to −7.1 ‰ for Mascall (n = 101, 10 taxa), and − 12.2 ‰ to −8.5 ‰ for the Rattlesnake formation (n = 49, 7 taxa) (Table 2, Fig. 2). The Rattlesnake formation has the narrowest $\delta^{13}C$ range but a similar $\delta^{13}C$ median (−10.5 ‰) and $\delta^{13}C$ mean (−10.4 ± 0.9 ‰) compared to the other fossil assemblages. When considering all specimens, mammals from the John Day, Mascall, and Rattlesnake Formations have similar $\delta^{13}C$ distributions (Levene test: p = 0.08). An ANOVA and Tukey test found that the Mascall Formation has a significantly greater mean $\delta^{13}C$ than the John Day Formation (p = 0.029). However, the Mascall and Rattlesnake did not have statistically different mean $\delta^{13}C$ (p = 0.99), nor did the John Day Formation and the Rattlesnake Formation (p = 0.100).

Estimates of past diets based on reconstructed atmospheric $\delta^{13}C$ show that all three communities fall within the bounds that were

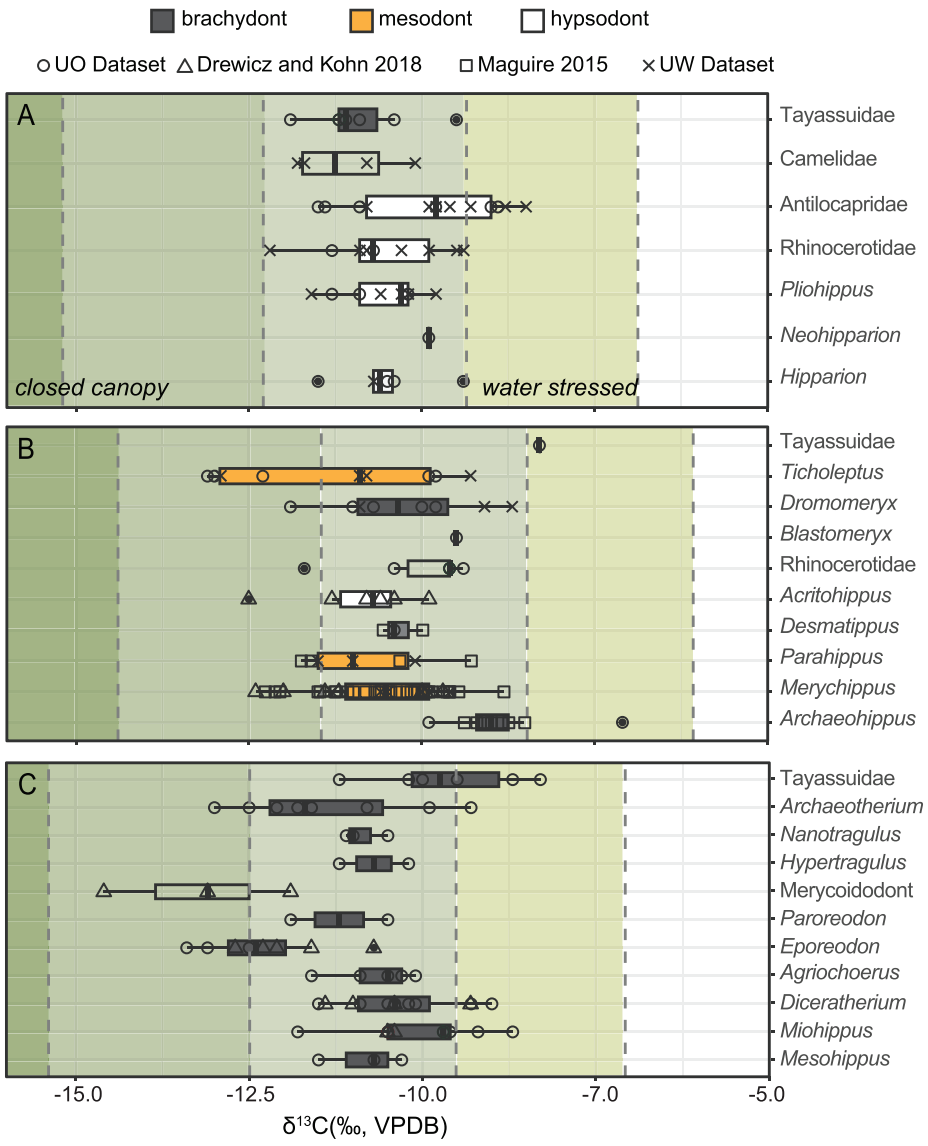

Fig. 2. Combined carbon data and predicted dietary composition
$\delta^{13}C$ values of fossil tooth enamel samples from the Rattlesnake Formation (panel A), Mascall Formation (panel B), and the Turtle Cove Member of the John Day Formation (panel C). Data is from Maguire, 2015, Drewicz and Kohn, 2018, and samples from this study which were analyzed in the University of Oregon Stable Isotope Laboratory (UO dataset) and in the University of Wyoming Stable Isotope Facility (UW dataset). Boxplots are shaded to represent tooth height values for that genus from Janis et al., 2004 and the NOW database. Groups where the tooth height was not found or applicable do not have shaded boxes. Points represent measurements from individuals. For each box plot, the thicker vertical line represents the median, the box represents the interquartile range, and the lower and upper whisker lines represent 1.5 interquartile range. Measurements outside the 1.5 interquartile range are represented with solid points. Gray dashed lines represent boundaries between predicted diets in closed canopy to water-stressed C_3 environments. Predictions are based on $\delta^{13}C$ values from modern C_3 floras from Kohn, 2010 that were adjusted for diet-enamel enrichment and change in atmospheric $\delta^{13}C$ values through time (see supplemental for enrichment values and calculations).

estimated for a purely C_3 vegetation diet (Fig. 2). Additionally, all measurements fall above what we would expect for herbivores which rely on food from closed canopy systems. All three communities have some measurements that fall within the values expected for individuals occupying a water-stressed C_3 environment. Both the John Day and the Rattlesnake communities have more values within the water-stressed C_3 vegetation than the Mascall Formation, where only two specimens show $\delta^{13}C$ above the threshold of −8.5 ‰.

3.3. Within community comparisons

In the John Day Formation, the tayassuid specimens have the most positive mean $\delta^{13}C$ value (−9.7 ± 1.1 ‰) and the most positive individual value at −8.5 ‰. *Miohippus* has the next most positive mean $\delta^{13}C$ value (−10.0 ± 0.9 ‰). The most negative mean $\delta^{13}C$ value belongs to the unidentified merycoidodonts (−13.2 ± 1.4 ‰). *Eporeodon* has the second lowest mean $\delta^{13}C$ values (−12.3 ± 0.9 ‰) in the John Day Formation community (Fig. 2C). Levene's test did not find a significant difference in variance among the John Day formation taxa ($p = 0.51$). ANOVA and Tukey test results show that there are eight taxon pairs in the John Day Formation that have significantly different mean $\delta^{13}C$ values (ANOVA $p < 0.0001$; Tukey test results Table 3). The mean $\delta^{13}C$ of unidentified merycoidodonts is significantly lower than both *Agriochoerus* ($p = 0.002$) and *Diceratherium* ($p < 0.001$). *Eporeodon* was found

Table 2
Mean, Median, standard deviation, and range of $\delta^{13}C$ (‰), and number of specimens measured for each formation. These values are based on measurements taken for this study, Maguire, 2015, and Drewicz and Kohn, 2018. Mean, Median, standard deviation, and range of $\delta^{18}O$ (‰), and number of specimens measured for each formation from $\delta^{18}O_{UO}$.

Formation	n	Median $\delta^{13}C$ (‰)	Mean $\delta^{13}C$ (‰)	S.D. (‰)	Range (‰)
Rattlesnake	49	−10.5	−10.4	0.88	3.7
Mascall	101	−10.4	−10.42	1.07	6
John Day	62	−10.7	−10.87	1.28	6.3
	n	**Median $\delta^{18}O$ (‰)**	**Mean $\delta^{18}O$ (‰)**	**S.D. (‰)**	**Range (‰)**
Rattlesnake	23	−7.5	−7.29	1.99	8
Mascall	21	−6.1	−6.25	2.09	7.4
John Day	47	−6.9	−6.59	2.11	9.3

to have a significantly lower $\delta^{13}C$ mean value than *Diceratherium* ($p = 0.0013$), *Miohippus* ($p = 0.0003$), and the tayassuid specimens ($p = 0.0001$). Additionally, the tayassuid specimens have significantly higher mean $\delta^{13}C$ than the unidentified merycoidodonts ($p < 0.0001$) and *Archaeotherium* ($p = 0.004$). *Archaeotherium* has the largest range of values (3.7 ‰) in $\delta^{13}C$ with some individuals overlapping with *Eporeodon*.

In the Mascall Formation community, *Archaeohippus* has the most positive mean $\delta^{13}C$ value (−8.9 ± 0.8 ‰) and also has the most positive individual $\delta^{13}C$ value at −7.1 ‰. The tayassuid specimen has the second most positive individual $\delta^{13}C$ value at −8.3 ‰. *Ticholeptus* has the most negative mean $\delta^{13}C$ value (−11.3 ± 1.5 ‰), the most negative individual $\delta^{13}C$ value (−13.1 ‰), and the widest range of $\delta^{13}C$ values (3.8 ‰) (Fig. 2B). A Levene's test found that Mascall taxa have significantly different variances in $\delta^{13}C$ ($p = 0.0084$). Kruskal-Wallis rank sum test and the following Wilcoxon rank-sum test found that *Archaeohippus* has a $\delta^{13}C$ distribution that significantly differs from all other taxa expect *Dromomeryx* (mean − 10.3 ‰ $\delta^{13}C$) (Kruskal-Wallis $x^2(7) = 26.131$, $p = 0.0005$; Wilcoxon rank-sum results Table 4). *Acritohippus* (mean − 10.9 ‰ $\delta^{13}C$) was previously found to differ isotopically from *Archaeohippus* by Maguire (2015) and this finding holds true with our additional samples. *Ticholeptus* and *Archaeohippus* were also found to differ significantly ($p = 0.012$).

In the Rattlesnake Formation, the antilocaprid samples have the most positive mean $\delta^{13}C$ value (−9.9 ± 1.0 ‰) and the most positive individual $\delta^{13}C$ value at −8.5 ‰. The antilocaprid samples also have the highest $\delta^{13}C$ range (3.0 ‰) compared with the other taxon sampled, but they also have the highest sample size ($n = 13$). The camelid specimens have the most negative mean $\delta^{13}C$ value (−11.1 ± 0.8 ‰), but the most negative individual $\delta^{13}C$ value (−12.2 ‰) belongs to a Rhinocerotidae specimen (Fig. 2A). Levene's test did not find a significant difference in $\delta^{13}C$ variance among the Rattlesnake Formation taxa ($p = 0.69$). Additionally, the Rattlesnake Formation taxa do not have significantly different mean $\delta^{13}C$ values from one another ($p = 0.07$).

3.4. Oxygen isotopes

All summary statistics for $\delta^{18}O$ of individual taxa can be found in Supplemental material 4, and Fig. 3 shows $\delta^{18}O$ results. We differentiate $\delta^{18}O$ from samples analyzed at University of Oregon ('$\delta^{18}O_{UO}$') from those analyzed at University of Wyoming ('$\delta^{18}O_{UW}$'). When the samples of the same taxon and geological unit are represented in both datasets, including *Dromomeryx* and *Ticholeptus* from Mascall Formation, Antilocapridae, *Hipparion*, *Pliohippus*, and Rhinocerotidae from Rattlesnake Formation, taxon mean $\delta^{18}O_{UO}$ are higher by 2.9 ‰ compared to taxon mean $\delta^{18}O_{UW}$. Specimen JODA 6450 is the only individual specimen analyzed in both laboratories, yielding a similar difference of 2.7 ‰ in its oxygen isotope composition ($\delta^{18}O_{UO} = -5.4$ and $\delta^{18}O_{UW} = -8.1$ ‰). See the Discussion for further consideration of the apparent spacing between $\delta^{18}O_{UO}$ and $\delta^{18}O_{UW}$ datasets, but out of an abundance of caution we consider $\delta^{18}O_{UO}$ only for the following statistical comparisons (Chesson et al., 2019).

When considering all specimens, mammals from the John Day, Mascall, and Rattlesnake Formations have similar $\delta^{18}O$ distributions (Levene test: $p = 0.72$), and the formations were not found to have significantly different mean $\delta^{18}O$ from one another ($p = 0.23$). Some

Table 3
Tukey test *p*-values on combined $\delta^{13}C$ (‰) data from this study, Maguire, 2015, and Drewicz and Kohn, 2018 from the Turtle Cove Member of the John Day Formation. Top row represents the species in the pairwise comparison.

John Day	1	2	3	4	5	6	7	8	9	10
1. *Agriochoerus*										
2. *Archaeotherium*	0.9634									
3. *Diceratherium*	0.9998	0.3603								
4. *Eporeodon*	0.1106	0.6613	**0.0013**							
5. *Hypertragulus*	1.0000	0.9975	1.0000	0.5365						
6. Merycoidodont	**0.0208**	0.1563	**0.0008**	0.9362	0.1415					
7. *Mesohippus*	1.0000	0.9985	0.9989	0.4361	1.0000	0.0961				
8. *Miohippus*	0.9672	0.1204	0.9993	**0.0003**	0.9967	**0.0002**	0.9605			
9. *Nanotragulus*	1.0000	0.9991	0.9981	0.4701	1.0000	0.1063	1.0000	0.9488		
10. *Paroreodon*	0.9998	1.0000	0.9776	0.9160	1.0000	0.4195	1.0000	0.8619	1.0000	
11. Tayassuidae	0.7613	**0.0438**	0.9245	**0.0001**	0.9482	**0.0001**	0.7783	0.9996	0.7488	0.6270

Table 4
Wilcoxon rank-sum test p-values on combined data from this study, Maguire, 2015, and Drewicz and Kohn, 2018 from the Mascall Formation. Top row represents the species in the pairwise comparison.

	1	2	3	4	5	6	7
1. *Acritohippus*							
2. *Archaeohippus*	**0.0151**						
3. *Desmatippus*	0.5244	0.0424					
4. *Dromomeryx*	0.6095	0.0834	0.9553				
5. *Merychippus*	0.5641	**0.0003**	0.7600	0.7059			
6. *Parahippus*	1.0000	**0.0098**	0.6889	0.5244	0.7059		
7. Rhinocerotidae	0.2351	**0.0424**	0.5244	0.7059	0.1956	0.5244	
8. *Ticholeptus*	0.7600	**0.0118**	0.6745	0.4512	0.4456	0.7075	0.2418

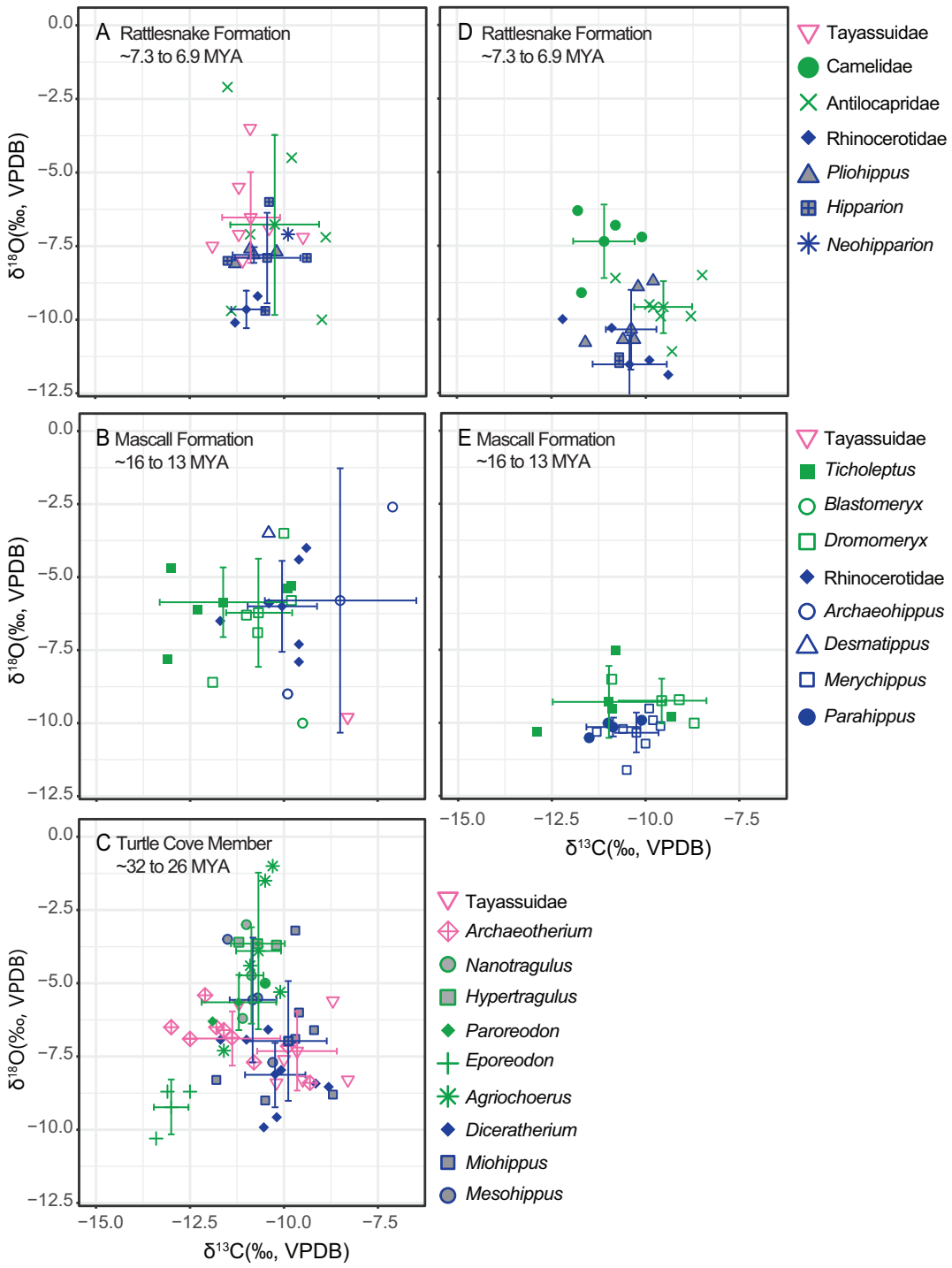

Fig. 3. New measurements for this study
Fossil tooth enamel $\delta^{13}C$ and $\delta^{18}O$ values from $\delta^{18}O_{UO}$ (panels A,B,C) and $\delta^{18}O_{UW}$ (panels D,E). Symbols represent different species from the Rattlesnake Formation (panels A,D), Mascall Formation (panels B,E), and John Day Formation (panel C). Lines indicate the standard deviation around the mean. Points are roughly colored by taxonomic order with blue representing Perissodactyla, green representing Artiodactyla, pink representing the omnivorous Tayassuidae and Archaetherium. (For interpretation of the references to colour in this figure legend, the reader is referred to the web version of this article.)

taxa that have significantly different mean $\delta^{13}C$ also differ in average $\delta^{18}O$ values. Levene tests were non-significant for differences in $\delta^{18}O$ variances among taxa for all formations (John Day $p = 0.26$, Mascall $p = 0.062$, Rattlesnake $p = 0.25$). Both Fig. 3 and ANOVA results indicated that both the Rattlesnake fauna ($p = 0.349$) and Mascall fauna ($p = 0.99$) do not have significantly different mean oxygen isotopic values from other taxa in the community.

In the John Day Formation, ANOVA and Tukey test results show that there are six taxon pairs differ significantly in $\delta^{18}O$ (Table 5). Many of these pairs include *Eporerodon* and *Agriochoerus*. *Eporeodon* differs from the other ungulates in having both low $\delta^{18}O$ (mean = −9.2 ± 0.9 ‰) (Fig. 3C). *Diceratherium* also has a low $\delta^{18}O$ (mean = −8.1 ± 1.1 ‰) compared with the other ungulates and is significantly lower than *Agriochoerus antiquus* ($\delta^{18}O = -3.9 \pm 2.6$ ‰) ($p = 0.0013$) and *Hypertragulus* ($\delta^{18}O = -3.7 \pm 0.1$ ‰) ($p = 0.028$). Additionally, *Agriochoerus antiquus* has a wide spread of $\delta^{18}O$ values (maximum = −7.3 ‰,

Table 5
Tukey test *p*-values on $\delta^{18}O$ (‰) measurements from $\delta^{18}O_{UO}$ from the Turtle Cove Member of the John Day Formation. Top row represents the species in the pairwise comparison.

Turtle Cove	1	2	3	4	5	6	7	8	9
1. *Agriochoerus*									
2. *Archaeotherium*	0.0541								
3. *Diceratherium*	**0.0013**	0.8524							
4. *Eporeodon*	**0.0016**	0.4732	0.9874						
5. *Hypertragulus*	1.0000	0.2523	**0.0279**	**0.0131**					
6. *Mesohippus*	0.9025	0.9605	0.3539	0.1559	0.9387				
7. *Miohippus*	0.0537	1.0000	0.9142	0.5500	0.2389	0.9489			
8. *Nanotragulus*	0.9991	0.5899	0.0763	**0.0355**	0.9988	0.9996	0.5643		
9. *Paroreodon*	0.9401	0.9908	0.6112	0.3042	0.9540	1.0000	0.9868	0.9997	
10. Tayassuidae	**0.0288**	1.0000	0.9933	0.7759	0.1559	0.8524	1.0000	0.3998	0.9481

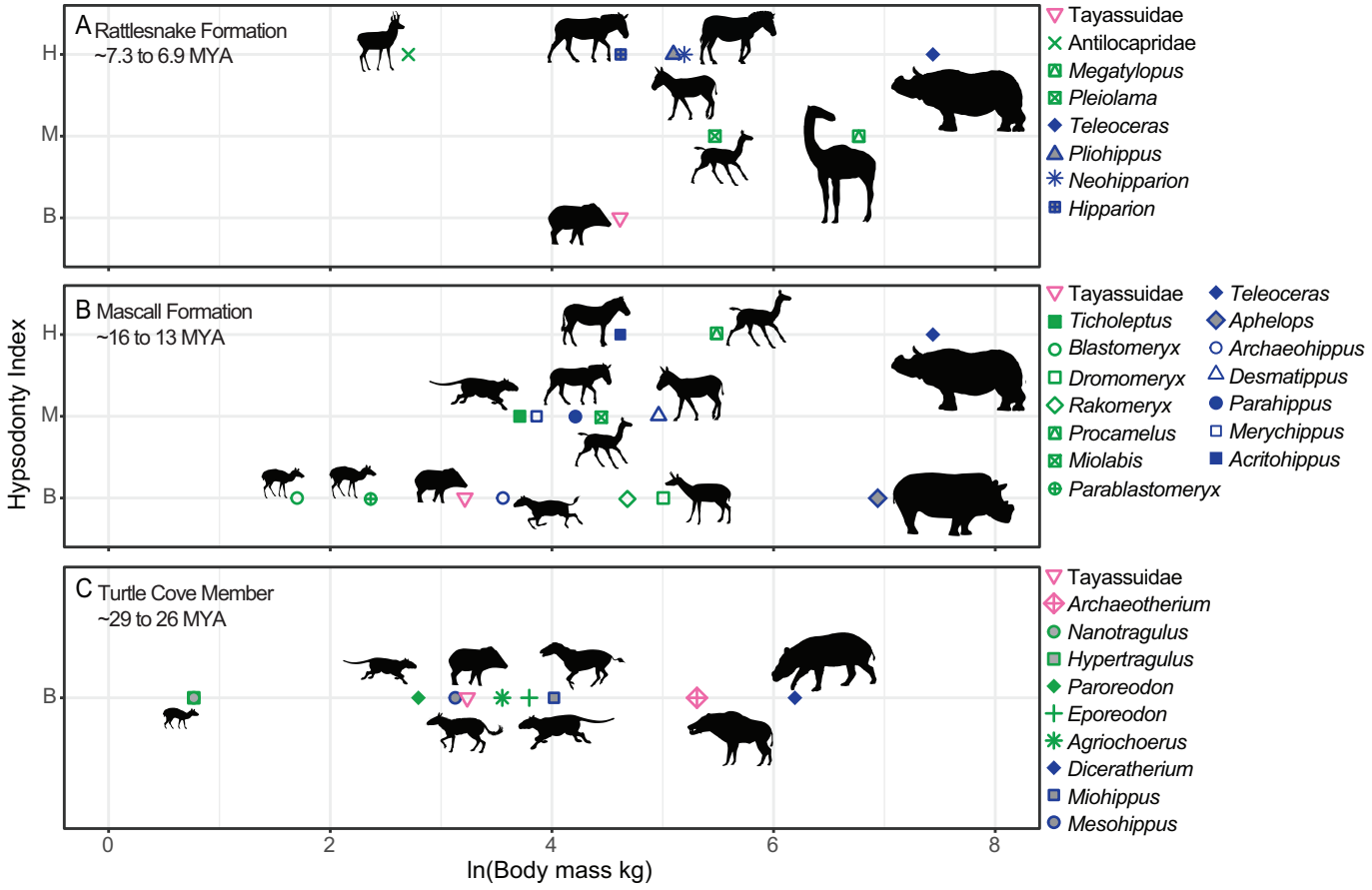

Fig. 4. Body mass and hypsodonty data
Tooth height and body mass (natural log of kg) estimates for extinct ungulate species from the Rattlesnake Formation (A), Mascall Formation (B), and John Day Formation (C). Hypsodonty categories are brachydont (B), mesodont (M), and hypsodont (H). Points are roughly colored by taxonomic order with blue representing Perissodactyla, green representing Artiodactyla, pink representing the omnivorous Tayassuidae and Archaetherium. (For interpretation of the references to colour in this figure legend, the reader is referred to the web version of this article.)

minimum = −1.0 ‰) and the most positive $\delta^{18}O$ values recorded in the community.

3.5. Hypsodonty and estimated body masses

Reported hypsodonty data indicate that the average tooth crown height increased through time in the Oregon ungulate communities (Fig. 4). All the ungulate species found within the Turtle Cove Member of the John Day Formation have brachydont teeth. In contrast, the Rattlesnake Formation hosts many equids with hypsodont teeth and the only ungulates with brachydont teeth are tayassuids. Body-mass estimates show a similar pattern with the John Day Formation and Mascall Formation hosting many more small-bodied ungulate species while the majority of taxa found in the Rattlesnake Formation have masses at or above 100 kg. The most functionally diverse ungulate community appears to be the Mascall Formation. It is diverse in number of species and in the spread of degree of hypsodonty and body mass. Few taxa overlap in either category in the Mascall Formation. Our $\delta^{13}C$ data paired with the reported hypsodonty data (Fig. 2) show no consistent pattern of brachydont taxa having lower average $\delta^{13}C$ than more hypsodont taxa.

4. Discussion

The large compilation of data we present for these three Oregon

fossil assemblages suggests that after the MMCO, ungulate diversity and dietary-niche partitioning changed likely in response to environmental dynamics. $\delta^{13}C$ data paired with the reported hypsodonty data provide the strongest evidence for this shift.

4.1. Niche partitioning in the Miocene of Oregon

In this study, the variation in trait combinations (i.e., body mass and tooth-crown height) paired with the isotopic evidence, suggest that ungulate ecology, and likely niche partitioning, in the Oregon ungulate communities shifted during the Oligo-Miocene. Dietary-niche partitioning is thought to facilitate high species richness in ungulate communities by reducing competition (Pansu et al., 2022). Our results provide isotopic evidence that ungulates consumed isotopically different plant-food resources in the Turtle Cove Member of the John Day Formation and the Mascall Formation. Both the John Day Formation and the Mascall Formation have been reconstructed as a mosaic open-woodland landscape with a diversity of microhabitats available to terrestrial mammal species (Retallack et al., 2000; Retallack, 2009; Bestland et al., 2008; Samuels et al., 2015; Maguire, 2015). The complicated and heterogeneous landscape would have allowed for some organisms to consume plants from wooded, more well-shaded patches (lower $\delta^{13}C$) as well as more open patches (higher $\delta^{13}C$). The Miocene communities likely used common partitioning strategies observed in modern ungulate communities, including eating plants in different habitats, eating different plant parts, or eating plant material at different foraging heights (Pansu et al., 2022; Potter et al., 2022). The isotopic data provide evidence of resource partitioning that is not apparent from the tooth morphology and body size data alone.

4.1.1. John day Formation

In the Turtle Cove Member of the John Day Formation, the relatively lower $\delta^{13}C$ and $\delta^{18}O$ of the *Eporeodon* samples suggest that the dietary ecology of *Eporeodon* differed from other ungulates in the community, especially *Diceratherium, Miohippus,* and the Tayassuidae. *Diceratherium*, *Miohippus,* and members of the Tayassuidae, all have measurements with $\delta^{13}C$ values above our reconstructed cutoff for water-stressed C_3 plants. *Eporeodon* has measurements that are below the average $\delta^{13}C$ for C_3 (Fig. 2C).

Previous studies have suggested that *Eporeodon* has mesowear patterns consistent with mixed feeders or browsers that consumed a fair amount of grit (Mihlbachler and Solounias, 2006). *Diceratherium* and *Miohippus* have also been hypothesized as being browsing organisms given their brachydont molars and the mesowear patterns of *Miohippus* (Mihlbachler et al., 2011). Our $\delta^{13}C$ data, however, provide evidence that at these Oregon localities *Eporeodon* differed in its eating habits from both *Diceratherium* and *Miohippus* more than what would be expected given just morphological data. The relatively low average $\delta^{13}C$ for *Eporeodon* could reflect browsing in more densely vegetated areas or consuming more mature leaves. In contrast, *Miohippus* and *Diceratherium* could have been consuming more C_3 grass. This interpretation does agree with microwear patterns for *Miohippus,* which suggest that it consumed low-abrasion C_3 grass (Semprebon et al., 2016).

Comparing the results for all the Merycoidodontoidea taxa in the assemblage, especially *Agriochoerus antiquus* and *Eporeodon*, show that the merycoidodont group had diverse ecologies during this time. In our study, mean $\delta^{13}C$ for *A. antiquus* did not differ significantly from that of *Eporeodon* but it did have a significantly higher $\delta^{18}O$ than *Eporeodon* (Fig. 3C and Table 5). *Agriochoerus antiquus* from the White River Group in Nebraska had elevated $\delta^{18}O$ relative to the other organisms in the community, which is similar to our results (Boardman and Secord, 2013). However, in the White River group *A. antiquus* also had relatively higher $\delta^{13}C$ than the other organisms in the community, suggesting it fed in more open areas on the landscape (Boardman and Secord, 2013). Our results do support the suggestion that *A. antiquus* could have relied less on drinking for their water needs and our results suggest that *Eporeodon* did not share this tendency.

4.1.2. Mascall Formation

In the Mascall Formation, *Ticholeptus,* the only merycoidodontoid in the assemblage, has the lowest $\delta^{13}C$ in the community. This result is interesting, as past work suggested that *Ticholeptus* likely occupied more open habitats than other merycoidodontoids, based on its relatively higher-crowned teeth (Lander, 1998). While our isotopic evidence does not indicate closed-canopy habitat use, the wide range of $\delta^{13}C$ values, coupled with *Ticholeptus'* notably lower $\delta^{13}C$ values, suggests a diverse diet that incorporated a range of plant resources. These isotopic results agree with past suggestions that based on mesowear, *Ticholeptus* was a mixed feeder but still had browsing tendencies like the rest of the members of the Merycoidodontoidea (Mihlbachler and Solounias, 2006). Another mesowear and microwear study suggested that *Ticholeptus* was likely a fruit and leaf browser (Semprebon et al., 2019) which also would be consistent with our isotopic findings.

In contrast to *Ticholeptus, Archaeohippus* has some higher $\delta^{13}C$ values suggesting they consumed foods in drier environments or plant parts that have experienced more water stress. Because of its small body size and low crowned teeth, *Archaeohippus's* $\delta^{13}C$ values have been hypothesized to reflect a diet of crown or young leaves from low bushes as opposed to the C_3 grasses that would have grown in the more open part of the environment at the time (Maguire, 2015). Additionally, microwear patterns sporting large puncture-like pits suggest that *Archaeohippus* incorporated fruit into its diet (Semprebon et al., 2016) which also could explain the higher $\delta^{13}C$ values (Metcalfe, 2021). Paleobotanical and paleopedology evidence from the Mascall suggest a humid temperate climate with dry-warm summers similar to Mediterranean climates and cool winters similar to continental climates (Chaney, 1956; Chaney, 1959; Bestland et al., 2008; Dillhoff et al., 2009). This environment would have supported fruit and nut bearing trees which both *Ticholeptus* and *Archaeohippus* could have consumed.

Although past microwear evidence indicates that both *Ticholeptus* and *Archaeohippus* were frugivorous browsers (Semprebon et al., 2016, 2019), and morphological evidence suggests they were similar in size, our isotopic results indicate that it is likely that *Ticholeptus* and *Archaeohippus* consumed foods in different parts of the landscape. *Archaeohippus* likely relied on more open patches for food, while *Ticholeptus* consumed food from a range of closed to more open patches. Potentially, *Archaeohippus* had an ecology similar to the modern Southern Pudu (*Pudu pudu*), which prefers forests with thick understories for cover from predators, but feeds on young leaves, fruits, and flowers in forest edges and open shrublands (Jiménez, 2010). Although we found no isotopic evidence for thick closed canopies in the Mascall there likely were areas of thicker vegetation for smaller ungulates such as *Archaeohippus* to seek refuge when threatened (Chaney, 1956; Chaney, 1959).

4.1.3. Rattlesnake Formation

In contrast to the John Day and Mascall Formations, the $\delta^{13}C$ values suggest that the Rattlesnake Formation ungulates were eating isotopically similar foods. Additionally, the Rattlesnake fauna is more homogeneous in terms of body mass and tooth height compared with the Mascall Formation. Body mass and hypsodonty estimates show that within the Rattlesnake Formation, most of the ungulates were large bodied with mesodont or hypsodont teeth. The lack of isotopic variation, paired with the decrease in body mass and tooth height diversity, suggests that 1) the Rattlesnake Formation had a more homogeneous flora than pre MMCO localities, 2) the niche partitioning mechanisms shifted post MMCO, or 3) niche overlap increased between ungulates after the MMCO. A combination of these factors is also possible.

The post-MMCO change in ungulate community structure found in our study parallels the patterns seen in both modern environments and other fossil localities. Modern grazer-dominated communities have been shown to have higher niche overlap in plant taxa consumption than

browser dominated communities (Pansu et al., 2022) which our data seem to be consistent with. Plant taxa partitioning was also shown to be greater between species of different sizes (Pansu et al., 2022), which is also consistent with our data given that the Rattlesnake ungulate community has fewer small-bodied taxa. Additionally, most of the Rattlesnake Formation ungulates have hypsodont teeth, which have been shown to allow ungulates to eat a wide variety of plant material (Pardi and DeSantis, 2021). Unlike many browsing organisms, which often have specialized diets, organisms that have grazing adaptations (i.e., hypsodont teeth) are not limited by their morphology to just consuming grass, and can have broad diets that include browse (Pardi and DeSantis, 2021). Therefore, the diets of the ungulates in the Rattlesnake Formation could have been wide and varied, which would mix the plant isotopic signals and result in relatively homogeneous isotopic niches. For instance, antilocaprids today have high-crowned teeth but are known to consume a wide variety of plants with a preference for browse, sagebrush, and forbs (O'Gara, 1978). The Rattlesnake Formation Antilocapridae were likely similar to their modern-day counterparts. They are the only group with $\delta^{13}C$ above our estimated cutoff for water-stressed C_3 plants, and their higher values are consistent with *Antilocapra americana* collagen and scat sample $\delta^{13}C$ values collected in modern C_3 ecosystems (Feranec, 2007a, 2007b). Furthermore, the extinct peccaries *Mylohyus* and *Platygonus,* which are both found within the Rattlesnake Formation, have $\delta^{13}C$ evidence of broad dietary niches even at the local level (Pardi and DeSantis, 2021), supporting the idea that the isotopic signals we are seeing are the result of varied plant consumption over the landscape.

Ungulate niche overlap, however, is not just determined by morphology as it is further regulated by degree of competition between the members of the community. Given the isotopic overlap between the ungulates, competition for resources could have been low in the Rattlesnake ecosystem, reducing the need for niche partitioning. Feranec and MacFadden (2006) sampled ungulates from Clarendonian-aged assemblages in California and Florida, and found isotopic evidence for niche partitioning in Florida had but not in California. They suggested that along with potential vegetational differences, the decreased taxonomic diversity at the Black Hawk Ranch site in California could have reduced the need for resource partitioning. The Rattlesnake fauna is similarly lower in taxonomic diversity than the John Day and Mascall faunas. However, herbivore competition is complex and is affected by climate-regulated food abundance, landscape disturbances, and predation pressures, all of which, therefore, can cause changes in niche overlap (Pansu et al., 2022). Additionally, there are many ways that ungulates in modern African environments avoid competition through dietary niche partitioning, with some being more easily detected using stable isotopes (e.g., consuming C_3 vs C_4 plants, or plants in highly different microclimates; Cerling et al., 2003; Cerling et al., 2015), while others are more difficult to detect in extinct communities using stable isotopes (e.g., daily temporal partitioning, plant height partitioning, and plant species selection based on nutritional value). It is possible that because of the shift to a more grazer-dominated ungulate community, the Rattlesnake community relied on different and harder to-detect partitioning strategies to reduce dietary competition, than those that dominated the John Day and Mascall ecosystems before.

Future studies could shed additional light on the community structure of the Rattlesnake fauna. In other late Miocene localities, horses, and especially *Neohipparion* tend to have higher $\delta^{13}C$ values than other ungulates in the community (Feranec and MacFadden, 2006; Kita et al., 2014; Nguy and Secord, 2022). In our study, we sampled only one *Neohipparion*, and more samples in the future could show similar trends. Additionally, many of the fossils sampled for this study are hard to identify below the family level and may contain multiple species, which would mask any species-level dietary differences. This could be the case with the antilocaprid specimens from the Rattlesnake Formation, which have been identified as either *Ilingoceras* or *Sphenophalos* (Fremd, 2010). Furthermore, the Rattlesnake Formation has a depositional environment that is different from both the Mascall and John Day Formations, possibly introducing some taphonomic biases. Compared to the earlier deposits, the Rattlesnake Formation consists of coarser material such as sandstones and conglomerates (Martin and Fremd, 2001), which would suggest an environment with a lower likelihood of preserving material from smaller ungulates. Work in the future could sample other late Miocene assemblages in the Pacific Northwest, or sample other material from the Rattlesnake Formation, to see if the ungulates sampled in this study accurately represent the landscape.

4.2. Diversity changes, morphological changes, and environmental change

Our study provides evidence that the ungulate communities in Oregon experienced similar ecological changes that have been documented for the Miocene communities of the Great Plains (Janis et al., 2004), including a reduction in diversity at the end of the Miocene, which strongly impacted small-bodied browsing taxa. For instance, before the MMCO, the John Day Formation ungulate community had a high diversity of smaller-bodied ungulates with low-crowned teeth. The isotopic evidence suggests that although the various taxa look morphologically similar, they were consuming different plant resources or plant parts, such as *Eporeodon* consuming plant resources with lower $\delta^{13}C$ than other taxa. The $\delta^{13}C$ values from the ungulates agree with past paleosol indicators that the environment during the time of the Turtle Cove member of the John Day Formation was most likely a mix of open and wooded habitats (Retallack, 2004), as none of the $\delta^{13}C$ values represent a closed canopy environment and only some $\delta^{13}C$ values are consistent with a diet of water-stressed plants.

In contrast to the John Day Formation, the Mascall Formation (~16–13 Ma; Maguire et al., 2018) supports a higher diversity of ungulates with varied body masses and tooth morphologies. The isotopic data suggest a complex ecological community with members like *Ticholeptus* having wide dietary niches. Additionally, the isotopic data paired with past microwear evidence (Semprebon et al., 2016) suggests that *Archaeohippus* selected browse and fruit in more open patches of the landscape. Previous work in this formation suggested that this was a wet period in the history of Oregon and the climate was humid with warm-dry summers and wet-cool winters (Bestland, 2008), with the majority of rainfall occurring during the winter (Kukla et al., 2022). The ungulate stable carbon isotopic evidence does support this interpretation of the climate as very few ungulates have values consistent with consuming large amounts of water-stressed C_3 plants.

The ungulate community found in the Rattlesnake assemblage is markedly different from the communities found in the other two formations. Our isotopic data shows a much more limited range in $\delta^{13}C$ values compared with the other two formations suggesting more homogeneous vegetation than the previous two formations. Fossil evidence, such as faunal presence of boreal organisms, beavers, and petrified wood fragments, do support the existence of forested patches with some riparian and aquatic environments in the lower parts of the formation (Samuels and Zancanella, 2011; Samuels and Cavin, 2013). The upper part of the section contains paleosols that have been interpreted to show a transition from these riparian woodlands/meadows to tall grasslands, and arid sagebrush steppe, much like today's ecosystem (Retallack et al., 2002). The isotopic evidence from our samples, however, suggests that the C_3 vegetation consumed by the ungulates sampled had similar $\delta^{13}C$ values and was likely not from dense forested environments or extremely arid environments.

Our data also suggests that the Rattlesnake Formation had a more homogeneous ungulate community both morphologically and isotopically. Most notable is the absence of small-bodied ungulates with brachydont teeth. Maguire (2015) found isotopic evidence that in the Mascall Formation the small equid *Archaeohippus* had a narrow diet and suggested that this contributed to its extinction in the region shortly after the MMCO. In contrast, our results show that *Ticholeptus,* which also disappears from the landscape after the MMCO, has quite a large

range of $\delta^{13}C$ values. Body size could have also played a role in these extinctions as both *Archaeohippus* and *Ticholeptus* are smaller than many of the other ungulates in the Mascall community. The cooler climate and open habitats might have impacted the smaller-bodied ungulates, not only because of their diet, but also because of the stresses of living in an open landscape.

The volcanic and tectonic activity of Oregon has resulted in a more heterogeneous landscape than the Great Plains and this has been the case for millions of years. However, our work suggests that ungulate communities in Oregon still experienced a reduction in dietary and morphological diversity despite the suggestion that the landscape was more heterogeneous. Further work could investigate whether the heterogeneous landscape of Oregon allowed some smaller-bodied browsers to persist longer than they did in the Great Plains.

4.3. Oxygen isotopes and methodological considerations

$\delta^{18}O_{UO}$ taxon means are higher than $\delta^{18}O_{UW}$ taxon means for taxa represented in both datasets from the same geologic unit ($n = 6$). This finding provides an opportunity to explore the potential consequences for compiling tooth enamel $\delta^{18}O$ datasets associated with of differing tooth enamel sampling and pretreatments, analytical method, as well as phosphoric acid quality and digestion temperature (Passey et al., 2007; Demény et al., 2019; Chesson et al., 2019).

$\delta^{18}O_{UO}$ and $\delta^{18}O_{UW}$ datasets include the same taxa and geological units but, except for JODA 6450, not the same individual specimens. If $\delta^{18}O_{UO}$ and $\delta^{18}O_{UW}$ both reflect the original biogenic compositions, specimens included in each dataset include individual animals associated with different controls on body water $\delta^{18}O$ (and therefore tooth enamel $\delta^{18}O$) (Kohn, 1996). Variation between individuals could be the result of climatic or hydrological conditions, drinking and dietary behaviors, differences in geological age, environmental contexts, or behavioral variation among distinct species within groups identified only to genus or family level. However, Maguire et al. (2015) did compare $\delta^{13}C$ and $\delta^{18}O$ values for *Acritohippus* samples from the lower unit, middle unit, and upper unit of the Mascall Formation and found no difference between the values. We also do not find consistent differences or patterns in $\delta^{18}O$ across stratigraphic units or locality (Supplemental material 5). The difference between $\delta^{18}O_{UO}$ and $\delta^{18}O_{UW}$ of the JODA 6450 specimen could reflect sampling different locations of the crown and biogenic intra-tooth $\delta^{18}O$ variability (see Supplemental material 5). Given the consistent inter-lab $\delta^{18}O$ difference across multiple taxa, and the low likelihood of unintentional systematic sampling of specimens from distinct contexts or species, we consider other methodological factors underpinning apparent differences between the $\delta^{18}O_{UO}$ and $\delta^{18}O_{UW}$ datasets.

First, we consider the possibility of contamination of enamel samples, which must be free from contamination by non-enamel dental tissues (e.g., dentine) that less reliably retain original biogenic isotopic composition as well as non-tooth matrix (Koch et al., 1997). This study includes taxa with relatively thin enamel, such as *Ticholeptus*, suggesting the possibility that enamel samples analyzed in one of the labs could be contaminated with underlying dentine, but we consider this unlikely given that care was taken in both sampling efforts to minimize the possibility of dentine contamination during sampling (see Supplemental material 5). Another possibility is contamination by conservation glue, such as various acryloids, which are commonly used to protect the integrity of specimens in the collections sampled in this study. Samples included in the $\delta^{18}O_{UO}$ dataset were selected to avoid glued specimens where possible, and as a result were often tooth fragments that had received little conservation treatment. All $\delta^{18}O_{UO}$ dataset specimens were cleaned with acetone before drilling to minimize potential contamination.

Second, we consider differences in pretreatment methods. The $\delta^{18}O_{UW}$ dataset includes samples treated using an oxidizer (30 % hydrogen peroxide) prior to acetic acid, while the $\delta^{18}O_{UO}$ dataset includes samples treated using acetic acid only. Hydrogen peroxide has been widely used to remove organics from bioapatite samples, although this step that is unnecessary for carbon and oxygen isotope analysis of low-organic materials such as tooth enamel by phosphoric acid digestion and can instead potentially alter the isotopic composition of samples (Pellegrini and Snoeck, 2016). Nonetheless, tooth enamel treated using hydrogen peroxide followed by acetic acid, and replicates treated using acetic acid only, yield similar $\delta^{18}O$ (within 1 ‰) (Pellegrini and Snoek 2016), indicating that enamel pretreatment methods likely do not fully account for apparent offset between $\delta^{18}O_{UO}$ and $\delta^{18}O_{UW}$.

Third, we consider the influences of the phosphoric acid used to digest tooth enamel samples. Small differences in acid quality and concentration have relatively minimal effect on tooth enamel $\delta^{18}O$ (<0.5 ‰) (Demény et al., 2019), and reproducibility of measurements of standards analyzed alongside samples in both laboratories indicates acid quality is unlikely an issue. Acid digestion temperature, however, is known to have a larger effect on $\delta^{18}O$, and is especially important to consider in paleontological studies given that temperature-dependent acid fractionation of fossilized tooth enamel becomes increasingly different from calcites at higher digestion temperatures (Passey et al., 2007; Kusaka and Nakano, 2014). $\delta^{18}O_{UO}$ values were corrected for temperature-dependent acid fractionation using the apparent fractionation factor (α^*) for non-modern tooth enamel digested at 70 °C from Kusaka and Nakano (2014). In principle, this correction ensures that $\delta^{18}O_{UO}$ are equivalent to $\delta^{18}O_{UW}$, which have not been corrected for temperature-dependent acid fractionation. It is assumed that temperature-dependent acid fractionation of tooth enamel is the same as the calcite standards for reactions at room temperature, based on that assumption for reactions at 25 °C (Passey et al., 2007). It is possible that temperature-dependent oxygen isotope acid fractionation differs from assumed values across the digestion temperatures used in this study, although investigating this further lies beyond the scope of this study. We note, however, that the observed offsets between $\delta^{18}O_{UW}$ and $\delta^{18}O_{UO}$ exceeds the maximum temperature-dependent acid fractionation $\delta^{18}O$ difference of 1.5 ‰ reported by Passey et al. (2007), and it is also greater than the interpretative difference cutoff of 1.6 ‰ $\delta^{18}O$ suggested by Chesson et al. (2019), indicating that acid fractionation likely does not fully account for apparent differences between $\delta^{18}O_{UO}$ and $\delta^{18}O_{UW}$.

We suggest that multiple factors, potentially including the combined effects of pretreatment and acid temperature, likely contribute to the apparent spacing of $\delta^{18}O_{UW}$ and $\delta^{18}O_{UO}$ data, though further exploration lies beyond the scope of this study. Considering each dataset separately, comparisons of $\delta^{18}O$ across taxa or geologic units can provide meaningful information on biogenic patterns. For example, rhinocerotids that are generally expected to be obligate drinkers have lower $\delta^{18}O$ than camelids and antilocaprids, which we would expect to be less reliant on meteoric water given their extant counterparts (Fig. 3).

5. Conclusions

Our work shows the strength of combining isotopic analyses with morphological inferences for detecting ecological changes in extinct communities. We found isotopic evidence in both the Mascall Formation and Turtle Cove Member of the John Day Formation that ungulates were partitioning food resources in an ecosystem with no C_4 plants. Although various taxa look morphologically similar, they were consuming different plant resources or plant parts. Taken together, the isotopic evidence and morphological evidence shows that as the Oligo-Miocene progressed, the Oregon ungulate ecology changed. In both the Mascall Formation and Turtle Cove Member of the John Day Formation there is isotopic evidence that ungulates were partitioning food resources in an ecosystem with no C_4 plants. This study further provides evidence that before and during the Mid-Miocene Climatic Optimum, Oregon ungulates consumed different plant resources in a mosaic landscape. Our work suggests that as the environment dried and cooled after the Mid-Miocene Climatic Optimum the landscape became more homogeneous

and the ungulates on the landscape were eating isotopically similar C_3 plant-food resources. Additionally, the majority of taxa had low-crowned teeth before the Mid-Miocene Climatic Optimum and most had mesodont or hypsodont teeth after. Body size also likely played a role in determining extinction risk, as most small-bodied ungulates were lost after the Mid-Miocene Climatic Optimum. Our work suggests that in Oregon at the end of the Miocene, as global temperatures decreased and grasslands expanded, a more ecologically homogeneous herbivore community arose.

CRediT authorship contribution statement

Dana M. Reuter: Writing – review & editing, Writing – original draft, Visualization, Software, Project administration, Methodology, Investigation, Funding acquisition, Formal analysis, Data curation, Conceptualization. **Jensen M. Wainwright:** Writing – review & editing, Writing – original draft, Validation, Investigation, Data curation. **Jonathan M. Hoffman:** Writing – review & editing, Writing – original draft, Validation, Investigation, Data curation. **Mark T. Clementz:** Resources. **Scott A. Blumenthal:** Writing – review & editing, Validation, Supervision, Resources, Project administration, Conceptualization. **Samantha S.B. Hopkins:** Writing – review & editing, Validation, Supervision, Resources, Project administration, Conceptualization.

Declaration of generative AI and AI-assisted technologies in the writing process

During the final editing of this work the author(s) used OpenAI GPT-4o to improve the clarity of some sentences. After using this tool/service, the author(s) reviewed and edited the content as needed and take(s) full responsibility for the content of the published article.

Funding sources

This work was supported by a Geological Society of America graduate research grant and the University of Oregon Department of Earth Sciences Baldwin Scholarship (both to D.M.R.). D.M.R. was partially supported by NSF Postdoctoral Research Fellowships in Biology Program under Grant No. 2209402 (to D.M.R.) during the final manuscript writing. Some of the fossils sampled for this analysis were collected and curated with support from BLM grant #L19AC00079, and S.S.B.H. was partially supported during the manuscript writing by NSF EAR-2322803.

Declaration of competing interest

The authors declare that they have no known competing financial interests or personal relationships that could have appeared to influence the work reported in this paper.

Acknowledgements

We would like to thank N. Famoso, C. Schierup, and D. Flores for their assistance with the JODA collections and G. Perdue, M. Wilkins, and M. Hilbert for resources in the John Day region. We are grateful to R. Lisle for laboratory assistance. We would like to thank R. Terry and E. Davis for manuscript edits that improved the early versions of the manuscript. Additionally, we also thank the editor, R. Trayler, and an anonymous reviewer whose suggestions and comments helped us to improve the manuscript contents. Silhouettes in figures are from Phylopic.org.

Appendix A. Supplementary data

Supplementary data to this article can be found online at https://doi.org/10.1016/j.palaeo.2025.113173.

Data availability

The authors confirm that all data necessary for supporting the scientific findings of this paper have been provided.

References

Albright III, L.B., Woodburne, M.O., Fremd, T.J., Swisher III, C.C., MacFadden, B.J., Scott, G.R., 2008. Revised chronostratigraphy and biostratigraphy of the John Day Formation (Turtle Cove and Kimberly Members), Oregon, with implications for updated calibration of the Arikareean north American Land Mammal Age. J. Geol. 116, 211–237.

Badgley, C., Smiley, T.M., Terry, R., Davis, E.B., DeSantis, L.R.G., Fox, D.L., Hopkins, S.S. B., Jezkova, T., Matocq, M.D., Matzke, N., McGuire, J.L., Mulch, A., Riddle, B.R., Roth, V.L., Samuels, J.X., Strömberg, C.A.E., Yanites, B.J., 2017. Biodiversity and Topographic Complexity: Modern and Geohistorical Perspectives. Trends Ecol. Evol. 32, 211–226. https://doi.org/10.1016/j.tree.2016.12.010.

Barry, J.C., 1995. Faunal turnover and diversity in the terrestrial Neogene of Pakistan. In: Vrba, E.S., Denton, G.H., Partridge, T.C., Buckle, L.H. (Eds.), Paleoclimate and Evolution with Emphasis on Human Origins. Yale University Press, New Haven, pp. 115–134.

Bershaw, J., Cassel, E.J., Carlson, T.B., Streig, A.R., Streck, M.J., 2019. Volcanic glass as a proxy for Cenozoic elevation and climate in the Cascade Mountains, Oregon, USA. J. Volcanol. Geotherm. Res. 381, 157–167. https://doi.org/10.1016/j.jvolgeores.2019.05.021.

Bestland, E.A., Forbes, M.S., Krull, E.S., Retallack, G.J., Fremd, T., 2008. Stratigraphy, paleopedology, and geochemistry of the middle Miocene Mascall Formation (type area, Central Oregon, USA). PaleoBios 28, 41–61.

Bibi, F., 2007. Dietary niche partitioning among fossil bovids in late Miocene C3 habitats: Consilience of functional morphology and stable isotope analysis. Palaeogeography, Palaeoclimatology, Palaeoecology 253 (3–4), 529–538.

Blumenthal, S.A., Levin, N.E., Brown, F.H., Brugal, J.-P., Chritz, K.L., Harris, J.M., Jehle, G.E., Cerling, T.E., 2017. Aridity and hominin environments. Proc. Natl. Acad. Sci. U. S. A. 114, 7331–7336. https://doi.org/10.1073/pnas.1700597114.

Boardman, G.S., Secord, R., 2013. Stable isotope paleoecology of White River ungulates during the Eocene–Oligocene climate transition in northwestern Nebraska. Palaeogeography, Palaeoclimatology, Palaeoecology 375, 38–49. https://doi.org/10.1016/j.palaeo.2013.02.010.

Bryant, J.D., Froelich, P.N., 1995. A model of oxygen isotope fractionation in body water of large mammals. Geochimica et Cosmochimica Acta 59 (21), 4523–4537.

Cahoon, E.B., Streck, M.J., Koppers, A.A.P., Miggins, D.P., 2020. Reshuffling the Columbia River Basalt chronology—Picture Gorge Basalt, the earliest- and longest-erupting formation. Geology 48, 348–352. https://doi.org/10.1130/G47122.1.

Cerling, T.E., Harris, J.M., 1999. Carbon isotope fractionation between diet and bioapatite in ungulate mammals and implications for ecological and paleoecological studies. Oecologia 120, 347–363.

Cerling, T.E., Harris, J.M., MacFadden, B.J., Leakey, M.G., Quade, J., Eisenmann, V., Ehleringer, J.R., 1997. Global vegetation change through the Miocene/Pliocene boundary. Nature 389 (6647), 153.

Cerling, T.E., Harris, J.M., Passey, B.H., 2003. Diets of East African Bovidae based on stable isotope analysis. J. Mammal. 84 (2), 456–470.

Cerling, T.E., Andanje, S.A., Blumenthal, S.A., Brown, F.H., Chritz, K.L., Harris, J.M., Hart, J.A., Kirera, F.M., Kaleme, P., Leakey, L.N., Leakey, M.G., 2015. Dietary changes of large herbivores in the Turkana Basin, Kenya from 4 to 1 Ma. Proc. Natl. Acad. Sci. 112 (37), 11467–11472.

Chaney, R.W., 1956. The Ancient Forests of Oregon. Condon Lectures. Oregon State System of Higher Education, University of Oregon, Eugene, OR.

Chaney, R.W., 1959. Miocene Floras of the Columbia Plateau. Part I. Composition and Interpretation, 617. Carnegie Institute of Washington Contributions to Paleontology, pp. 1–134.

Chen, S.T., Smith, S.Y., Sheldon, N.D., Strömberg, C.A., 2015. Regional-scale variability in the spread of grasslands in the late Miocene. Palaeogeography, Palaeoclimatology, Palaeoecology 437, 42–52.

Chesson, L.A., Kenyhercz, M.W., Regan, L.A., Berg, G.E., 2019. Addressing data comparability in the creation of combined data sets of bioapatite carbon and oxygen isotopic compositions. Archaeometry 61, 1193–1206. https://doi.org/10.1111/arcm.12480.

Demény, A., Gugora, A.D., Kesjár, D., Lécuyer, C., Fourel, F., 2019. Stable isotope analyses of the carbonate component of bones and teeth: the need for methodological standardization. J. Archaeol. Sci. 109, 104979.

Dickinson, W.R., 2002. The Basin and Range Province as a Composite Extensional Domain. Int. Geol. Rev. 44, 1–38. https://doi.org/10.2747/0020-6814.44.1.1.

Dillhoff, R.M., Dillhoff, T.A., Dunn, R.E., Myers, J.A., Strömberg, C.A., 2009. Cenozoic Paleobotany of the John Day Basin, Central Oregon.

Drewicz, A.E., Kohn, M.J., 2018. Stable isotopes in large herbivore tooth enamel capture a mid-Miocene precipitation spike in the interior Pacific Northwest. Palaeogeogr. Palaeoclimatol. Palaeoecol. 495, 1–12. https://doi.org/10.1016/j.palaeo.2017.11.022.

Ehleringer, J.R., Cerling, T.E., 2002. C3 and C4 photosynthesis. Encyclopedia of global environmental change 2, 186–190.

Ehleringer, J.R., Sage, R.F., Flanagan, L.B., Pearcy, R.W., 1991. Climate change and the evolution of C4 photosynthesis. Trends Ecol. Evol. 6, 95–99.

Faith, J.T., 2018. Paleodietary change and its implications for aridity indices derived from δ18O of herbivore tooth enamel. Palaeogeography, Palaeoclimatology, Palaeoecology 490, 571–578. https://doi.org/10.1016/j.palaeo.2017.11.045.
Farquhar, G.D., Ehleringer, J.R., K.T., Hubick., 1989. Carbon isotope discrimination and photosynthesis. Annu. Rev. Plant Biol. 40, 503–537.
Feranec, R.S., 2003. Stable isotopes, hypsodonty, and the paleodiet of Hemiauchenia (Mammalia: Camelidae): a morphological specialization creating ecological generalization. Paleobiology 29, 230–242. https://doi.org/10.1666/0094-8373(2003)029<0230:SIHATP>2.0.CO;2.
Feranec, Robert S., 2007a. Ecological generalization during adaptive radiation: evidence from Neogene mammals. Evol. Ecol. Res. 9, 555–577.
Feranec, Robert S., 2007b. Stable carbon isotope values reveal evidence of resource partitioning among ungulates from modern C3-dominated ecosystems in North America. Palaeogeography, Palaeoclimatology, Palaeoecology 252, 575–585. https://doi.org/10.1016/j.palaeo.2007.05.012.
Fisher, R.V., Rensberger, J.M., 1972. Physical stratigraphy of the John Day Formation, Central Oregon, 101. University of California Publications in Geological Sciences, pp. 1–33.
Fox, J., Weisberg, S., 2019. An R Companion to Applied Regression, Third. ed. Sage, Thousand Oaks CA.
Fremd, T.J., 2010. Guidebook: SVP Field Symposium 2010 John Day Basin Field Conference.
Fricke, H.C., O'Neil, J.R., 1999. The correlation between 18O/16O ratios of meteoric water and surface temperature: its use in investigating terrestrial climate change over geologic time. Earth Planet. Sci. Lett. 170, 181–196. https://doi.org/10.1016/S0012-821X(99)00105-3.
Janis, C.M., 1988. An estimation of tooth volume and hypsodonty indices in ungulate mammals, and the correlation of these factors with dietary preference. In: Teeth Revisited: Proceedings of the VIIth International Symposium on Dental Morphology, 1988 (pp. 367-387). Memoirs de Musee d'Histoire naturalle du Paris.
Janis, C.M., Scott, K.M., Jacobs, L.L., Gunnell, G.F., Uhen, M.D. (Eds.), 1998. Evolution of tertiary mammals of North America: volume 1, terrestrial carnivores, ungulates, and ungulate like mammals, vol. 1. Cambridge University Press.
Janis, C.M., Damuth, J., Theodor, J.M., 2000. Miocene ungulates and terrestrial primary productivity: where have all the browsers gone? Proc. Natl. Acad. Sci. 97 (14), 7899–7904.
Janis, C.M., Damuth, J., Theodor, J.M., 2002. The origins and evolution of the north American grassland biome: the story from the hoofed mammals. Palaeogeography, Palaeoclimatology, Palaeoecology 177, 183–198.
Janis, C.M., Damuth, J., Theodor, J.M., 2004. The species richness of Miocene browsers, and implications for habitat type and primary productivity in the north American grassland biome. Palaeogeography, Palaeoclimatology, Palaeoecology 207, 371–398.
Jiménez, J.E., 2010. Southern pudu *Pudu puda* (Molina 1782). *Neotropical Cervidology: Biology and Medicine of Latin American Deer*. Funep & IUCN, Jaboticabal &, Gland, pp. 140–150.
Kartzinel, T.R., Chen, P.A., Coverdale, T.C., Erickson, D.L., Kress, W.J., Kuzmina, M.L., Rubenstein, D.I., Wang, W., Pringle, R.M., 2015. DNA metabarcoding illuminates dietary niche partitioning by African large herbivores. Proceedings of the National Academy of Sciences 112 (26), 8019–8024.
Koch, P.L., 2007. Isotopic Study of the Biology of Modern and Fossil Vertebrates. In: Stable Isotopes in Ecology and Environmental Science. John Wiley & Sons, Ltd, pp. 99–154. https://doi.org/10.1002/9780470691854.ch5.
Koch, P.L., Tuross, N., Fogel, M.L., 1997. The effects of sample treatment and diagenesis on the isotopic integrity of carbonate in biogenic hydroxylapatite. J. Archaeol. Sci. 24 (5), 417–429.
Kohn, M.J., 1996. Predicting animal δ18O: Accounting for diet and physiological adaptation. Geochim. Cosmochim. Acta 60, 4811–4829. https://doi.org/10.1016/S0016-7037(96)00240-2.
Kohn, M.J., 2010. Carbon isotope compositions of terrestrial C3 plants as indicators of (paleo) ecology and (paleo) climate. Proc. Natl. Acad. Sci. 107 (46), 19691–19695.
Kohn, M.J., Fremd, T.J., 2007. Tectonic Controls on Isotope Compositions and Species Diversification, John Day Basin, Central Oregon. PaleoBios.
Kukla, T., Rugenstein, J.K.C., Ibarra, D.E., Winnick, M.J., Strömberg, C.A., Chamberlain, C.P., 2022. Drier winters drove Cenozoic open habitat expansion in North America. AGU Advances 3 (2) e2021AV000566.
Kusaka, S., Nakano, T., 2014. Carbon and oxygen isotope ratios and their temperature dependence in carbonate and tooth enamel using a GasBench II preparation device. Rapid Commun. Mass Spectrom. 28 (5), 563–567.
Lander, B., 1998. Oreodontoidea. In: Janis, C.M., Scott, K.M., Jacobs, L.L. (Eds.), Evolution of Tertiary Mammals of North America, Terrestrial Carnivores, Ungulates, and Ungulatelike Mammals, vol. 1. Cambridge, Cambridge University Press, pp. 402–420.
Legendre, S., 1986. Analysis of mammalian communities from the late Eocene and Oligocene of southern France. Palaeovertebrata 16, 191–212.
Levin, N.E., Cerling, T.E., Passey, B.H., Harris, J.M., Ehleringer, J.R., 2006. A stable isotope aridity index for terrestrial environments. Proc. Natl. Acad. Sci. 103, 11201–11205. https://doi.org/10.1073/pnas.0604719103.
Loughney, K.M., Badgley, C., Bahadori, A., Holt, W.E., Rasbury, E.T., 2021. Tectonic influence on Cenozoic mammal richness and sedimentation history of the Basin and Range, western North America. Sci. Adv. 7, eabh4470. https://doi.org/10.1126/sciadv.abh4470.
Maguire, K.C., 2015. Dietary niche stability of equids across the mid-Miocene Climatic Optimum in Oregon, USA. Palaeogeography, Palaeoclimatology, Palaeoecology 426, 297–307. https://doi.org/10.1016/j.palaeo.2015.03.012.
Maguire, K.C., Samuels, J.X., Schmitz, M.D., 2018. The Fauna and Chronostratigraphy of the Middle Miocene Mascall Type Area, John Day Basin, Oregon. PaleoBios, USA, p. 35.
Martin, J., Fremd, T., 2001. Revision of the lithostratigraphy of the Hemphillian Rattlesnake units of Central Oregon. PaleoBios 21, 89.
Metcalfe, J.Z., 2021. C3 plant isotopic variability in a boreal mixed woodland: implications for bison and other herbivores. PeerJ 9, e12167.
Mihlbachler, M.C., Solounias, N., 2006. Coevolution of tooth crown height and diet in oreodonts (Merycoidodontidae, Artiodactyla) examined with phylogenetically independent contrasts. J. Mamm. Evol. 13 (1), 11–36.
Mihlbachler, M.C., Rivals, F., Solounias, N., Semprebon, G.M., 2011. Dietary Change and Evolution of horses in North America. Science 331, 1178–1181. https://doi.org/10.1126/science.1196166.
Mohr, M.T., Famoso, N.A., Samuels, J.X., Laib, A.C., Schmitz, M.D., 2025. U-Pb zircon geochronology and chronostratigraphy of the Eocene– Miocene John Day Formation of central and eastern Oregon, 21.
O'Gara, B.W., 1978. Antilocapra americana. Mamm. Species 90, 1–7.
Pansu, J., Hutchinson, M.C., Anderson, T.M., te Beest, M., Begg, C.M., Begg, K.S., Bonin, A., Chama, L., Chamaillé-Jammes, S., Coissac, E., Cromsigt, J.P.G.M., Demmel, M.Y., Donaldson, J.E., Guyton, J.A., Hansen, C.B., Imakando, C.I., Iqbal, A., Kalima, D.F., Kerley, G.I.H., Kurukura, S., Landman, M., Long, R.A., Munuo, I.N., Nutter, C.M., Parr, C.L., Potter, A.B., Siachoono, S., Taberlet, P., Waiti, E., Kartzinel, T.R., Pringle, R.M., 2022. The generality of cryptic dietary niche differences in diverse large-herbivore assemblages. Proc. Natl. Acad. Sci. 119, e2204400119. https://doi.org/10.1073/pnas.2204400119.
Pardi, M.I., DeSantis, L.R.G., 2021. Dietary plasticity of north American herbivores: a synthesis of stable isotope data over the past 7 million years. Proc. R. Soc. B Biol. Sci. 288, 20210121. https://doi.org/10.1098/rspb.2021.0121.
Passey, B.H., Cerling, T.E., Levin, N.E., 2007. Temperature dependence of oxygen isotope acid fractionation for modern and fossil tooth enamels. Rapid Communications in Mass Spectrometry: An International Journal Devoted to the Rapid Dissemination of Up-to-the-Minute Research in Mass Spectrometry 21 (17), 2853–2859.
Pellegrini, M., Snoeck, C., 2016. Comparing bioapatite carbonate pre-treatments for isotopic measurements: part 2 Impact on carbon and oxygen isotope compositions. Chem. Geol. 420, 88–96.
Pesek, M.E., Perez, N.D., Meigs, A., Rowden, C.C., Giles, S.M., 2020. Exhumation timing in the oregon cascade range decoupled from deformation, magmatic, and climate patterns. Tectonics 39. https://doi.org/10.1029/2020TC006078 e2020TC006078.
Pestle, W.J., Crowley, B.E., Weirauch, M.T., 2014. Quantifying Inter-Laboratory Variability in Stable Isotope Analysis of Ancient Skeletal remains. PloS One 9, e102844. https://doi.org/10.1371/journal.pone.0102844.
Potter, A.B., Hutchinson, M.C., Pansu, J., Wursten, B., Long, R.A., Levine, J.M., Pringle, R.M., 2022. Mechanisms of dietary resource partitioning in large-herbivore assemblages: A plant-trait-based approach. J. Ecol. 110, 817–832. https://doi.org/10.1111/1365-2745.13843.
Prothero, D.R., Hoffman, J.M., Foss, S.E., 2006. Magnetic stratigraphy of the upper Miocene (Hemphillian) Rattlesnake Formation, Central Oregon. PaleoBios 26, 37–42.
R Core Team, 2023. R: A Language and Environment for Statistical Computing. R Foundation for Statistical Computing, Vienna, Austria.
Reidel, S.P., Camp, V.E., Ross, M.E., Wolff, J.A., Martin, B.S., Tolan, T.L., Wells, R.E., 2013. The Columbia River Flood Basalt Province. Geological Society of America.
Retallack, G.J., 2004. Late Oligocene bunch grassland and early Miocene sod grassland paleosols from Central Oregon, USA. Palaeogeography, Palaeoclimatology, Palaeoecology 207 (3–4), 203–237.
Retallack, G.J., 2009. Cenozoic cooling and grassland expansion in Oregon and Washington. PaleoBios 28 (3), 89–113.
Retallack, G.J., Bestland, E.A., Fremd, T.J. (Eds.), 2000. Eocene and Oligocene Paleosols of Central Oregon, vol. 344. Geological Society of America.
Retallack, G.J., Tanaka, S., Tate, T., 2002. Late Miocene advent of tall grassland paleosols in Oregon. Palaeogeography, Palaeoclimatology, Palaeoecology 183, 329–354. https://doi.org/10.1016/S0031-0182(02)00250-X.
Rozanski, K., Araguás-Araguás, L., Gonfiantini, R., 1992. Relation between Long-Term Trends of Oxygen-18 Isotope Composition of Precipitation and climate. Science 258, 981–985. https://doi.org/10.1126/science.258.5084.981.
Samuels, J.X., Cavin, J., 2013. The earliest known fisher (Mustelidae), a new species from the Rattlesnake Formation of Oregon. J. Vertebr. Paleontol. 33 (2), 448–454.
Samuels, J.X., Albright, L.B., Fremd, T.J., 2015. The last fossil primate in North America, new material of the enigmatic *Ekgmowechashala* from the Arikareean of Oregon. Am. J. Phys. Anthropol. 158 (1), 43–54.
Semprebon, G.M., Rivals, F., Solounias, N., Hulbert, R.C., 2016. Paleodietary reconstruction of fossil horses from the Eocene through Pleistocene of North America. Palaeogeography, Palaeoclimatology, Palaeoecology 442, 110–127. https://doi.org/10.1016/j.palaeo.2015.11.004.
Semprebon, G.M., Rivals, F., Janis, C.M., 2019. The Role of Grass vs. Exogenous Abrasives in the Paleodietary patterns of north American Ungulates. Front. Ecol. Evol. 7. https://doi.org/10.3389/fevo.2019.00065.
Smiley, T.M., Bahadori, A., Rasbury, E.T., Holt, W.E., Badgley, C., 2024. Tectonic extension and paleoelevation influence mammalian diversity dynamics in the Basin and Range Province of western North America. Sci. Adv. 10, eadn6842. https://doi.org/10.1126/sciadv.adn6842.
Streck, M.J., Grunder, A.L., 1995. Crystallization and welding variations in a widespread ignimbrite sheet; the Rattlesnake Tuff, eastern Oregon, USA. Bull. Volcanol. 57 (3), 151–169.
Strömberg, C.A., 2011. Evolution of grasses and grassland ecosystems. Annu. Rev. Earth Planet. Sci. 39, 517–544.

Strömberg, C.A.E., Staver, A.C., 2022. The history and challenge of grassy biomes. Science 377, 592–593. https://doi.org/10.1126/science.add1347.
Takeuchi, A., Hren, M.T., Smith, S.V., Chamberlain, C.P., Larson, P.B., 2010. Pedogenic carbonate carbon isotopic constraints on paleoprecipitation: Evolution of desert in the Pacific Northwest, USA, in response to topographic development of the Cascade Range. Chem. Geol. 277 (3–4), 323–335.
The NOW Community, 2024. New and Old Worlds Database of Fossil Mammals (NOW). Licensed under CC BY 4.0. Retrieved 2024 from. https://nowdatabase.org/now/database/.
Tipple, B.J., Meyers, S.R., Pagani, M., 2010. Carbon isotope ratio of Cenozoic CO2: A comparative evaluation of available geochemical proxies. Paleoceanography 25 (3).
Vogado, N.O., Winter, K., Ubierna, N., Farquhar, G.D., Cernusak, L.A., 2020. Directional change in leaf dry matter δ 13C during leaf development is widespread in C3 plants. Annals of Botany 126 (6), 981–990.
Yakir, D., Deniro, M., Gat, J., 1990. Natural deuterium and oxygen-18 enrichment in leaf water of cotton plants grown under wet and dry conditions: evidence for water compartmentation and its dynamics. Plant Cell And Environment 13, 49–56. https://doi.org/10.1111/j.1365-3040.1990.tb01298.x.
Žliobaitė, I., Rinne, J., Tóth, A.B., Mechenich, M., Liu, L., Behrensmeyer, A.K., Fortelius, M., 2016. Herbivore teeth predict climatic limits in Kenyan ecosystems. Proc. Natl. Acad. Sci. 113 (45), 12751–12756.